Biogeosciences, 7, 1587–1606, 2010
www.biogeosciences.net/7/1587/2010/
doi:10.5194/bg-7-1587-2010

Biogeosciences

Air-Sea CO_2 fluxes in the Atlantic as measured during boreal spring and autumn

X. A. Padin[1], M. Vázquez-Rodríguez[1], M. Castaño[1], A. Velo[1], F. Alonso-Pérez[1], J. Gago[2], M. Gilcoto[1], M. Álvarez[3], P. C. Pardo[1], M. de la Paz[1], A. F. Ríos[1], and F. F. Pérez[1]

[1]Instituto de Investigaciones Marinas, CSIC, Eduardo Cabello 6, 36208 Vigo, Spain
[2]Instituto Español de Oceanografía (IEO. Vigo), Cabo Estai – Canido, Apartado 1552, 36200 Vigo, Spain
[3]Institut Mediterrani d'Estudis Avançats, CSIC-UIB, Miquel Marqués 21, 07190 Esporles, Spain

Received: 18 May 2009 – Published in Biogeosciences Discuss.: 12 June 2009
Revised: 21 April 2010 – Accepted: 23 April 2010 – Published: 18 May 2010

Abstract. A total of fourteen hydrographic cruises from 2000 to 2008 were conducted during the spring and autumn seasons between Spain and the Southern Ocean under the framework of the Spanish research project FICARAM. The underway measurements were processed and analysed to describe the meridional air-sea CO_2 fluxes (FCO_2) in the covered sector of the Atlantic Ocean. The data has been grouped into different biogeochemical oceanographic provinces based on thermohaline characteristics. The spatial and temporal distributions of FCO_2 followed expected distributions and annual trends reproducing the recent climatological ΔfCO_2 estimations with a mean difference of -3 ± 18 µatm (Takahashi et al., 2009). The reduction in the CO_2 saturation along the meridional FICARAM cruises represented an increase of 0.02 ± 0.14 mol m^{-2} yr^{-1} in the ocean uptake of atmospheric CO_2. The subtropical waters in both Hemispheres acted as a sink of atmospheric CO_2 during the successive spring seasons and as a source in autumn. The coarse reduction of the ocean uptake of atmospheric CO_2 observed in the North Atlantic Ocean was linked to conditions of negative phase of the North Atlantic Oscillation that prevailed during the FICARAM period. Surface waters in the North Equatorial Counter Current revealed a significant long-term decrease of sea surface salinity of -0.16 ± 0.01 yr^{-1} coinciding with a declination of -3.5 ± 0.9 µatm yr^{-1} in the air–sea disequilibrium of CO_2 fugacity and a rise of oceanic CO_2 uptake of -0.09 ± 0.03 mol m^{-2} yr^{-1}. The largest CO_2 source was located in the equatorial upwelling system. These tropical waters that reached emissions of 0.7 ± 0.5 and 1.0 ± 0.7 mol m^{-2} y^{-1} in spring and autumn, respectively, showed an interannual warming of 0.11 ± 0.03 °C yr^{-1} and a wind speed decrease of -0.58 ± 0.14 m s^{-1} yr^{-1} in spring cruises which suggest the weakening of upwelling events associated with warm El Niño – Southern Oscillation episodes. Contrary the surface waters of the Patagonian Sea behaved as an intense sink of CO_2 in March and November. The oceanic waters of the convergence of Falkland and Brazil Currents showed the strongest CO_2 absorption with a rate of -5.4 ± 3.6 mol m^{-2} yr^{-1} in November. The Southern Oceans sampled in the Drake Passage behave as an average uptake rate of -1.1 ± 0.9 mol m^{-2} yr^{-1} while the distal shelf of the Livingston Island acted as a slight source of CO_2 to the atmosphere.

Correspondence to: X. A. Padin
(padin@iim.csic.es)

1 Introduction

The CO_2 emissions associated with human activity, such as fossil fuel burning, changes in land-use or cement production, have increased atmospheric CO_2 concentrations (Keeling and Whorf, 2000; Houghton, 2003) from pre-industrial levels (∼270 ppm; parts per million of volume) to present-day ones, above 384 ppm (Solomon et al., 2007). Despite current total CO_2 emissions to the atmosphere of ∼9.1 PgC yr^{-1} (Canadell et al., 2007) only half of them are retained in the atmospheric reservoir (Sarmiento and Gruber, 2002; Sabine et al., 2004). Oceanic and terrestrial ecosystems sequestrate important amounts of CO_2, thus reducing atmospheric CO_2 accumulation. The combined storage of land and oceans mitigates significantly the rate of global warming by quenching the global temperatures sensed in the biosphere (Siegenthaler and Sarmiento, 1993).

Table 1. Information of the FICARAM cruises.

Cruise	Ship	Date	Latitude range
FICARAM 1	*R/V Hespérides*	Oct–Nov, 2000	36.5° N–11.1° S
FICARAM 2	*R/V Hespérides*	Mar–Apr, 2001	40° N–55.1° S
FICARAM 3	*R/V Hespérides*	Oct–Nov, 2001	36.6° N–7.8° S
FICARAM 4	*R/V Hespérides*	Mar–Apr, 2002	36.0° N–51.0° S
FICARAM 5	*R/V Hespérides*	Oct–Nov, 2002	37.4° N–23.1° S
FICARAM 6	*R/V Hespérides*	Apr, 2003	37.1° N–19.1° N
FICARAM 7	*R/V Hespérides*	Oct–Nov, 2004	37.3° N–55.1° S
FICARAM 8	*R/V Hespérides*	Oct–Nov, 2005	36.4° N–53.2° S
FICARAM 9	*R/V Hespérides*	Mar–Apr, 2006	32.4° N–55.1° S
FICARAM 10	*R/V Las Palmas*	Oct–Nov, 2006	37.4° N–53.2° S
FICARAM 11	*R/V Las Palmas*	Mar–May, 2007	37.5° N–54.8° S
FICARAM 12	*R/V Las Palmas*	Oct–Nov, 2007	36.0° N–62.9° S
FICARAM 13	*R/V Las Palmas*	Mar–Apr, 2008	37.4° N–55.1° S
FICARAM 14	*R/V Las Palmas*	Oct–Nov, 2008	37.5° N–62.9° S

Notwithstanding its importance, air-sea CO_2 fluxes (FCO_2) are constrained rather poorly and introduce large uncertainties in global carbon budget estimates, particularly at interannual scales (Keeling et al., 1995; Francey et al., 1995; Battle et al., 2000, Schuster et al., 2009). This stems from the scarcity of in situ FCO_2 measurements and from the lack of time-series records. In order to improve our understanding of the ocean CO_2 uptake, it is essential to constrain the uncertainties associated with air-sea CO_2 fluxes (FCO_2) estimates both geographically and temporally. The Spanish project FICARAM (Air-sea CO_2 fluxes along meridional tracks in the Atlantic Ocean), was part of an international effort to carry out extensive in situ measurements at oceanic basin scales using available ship-potential. The FICARAM project was developed as repeat VOS line within the framework of larger European projects such as CAVASSOO (Carbon Variability Studies by Ships Of Opportunity) and CARBOOCEAN (Marine Carbon Sources and Sinks Assessment). The surface CO_2 observations collected during FICARAM are part of databases compiled by the projects CARBOOCEAN and SOCAT (Surface Ocean CO_2 Atlas).

The FICARAM cruises (Table 1) were carried out taking advantage of bi-annual ship tracks between Spain and the Antarctic from 2000 to 2008 providing a unique opportunity to get a quasi-synoptic view of a meridional transect in both the North and South Atlantic Oceans. These high-resolution observations helped showing the distribution over seasonal and long-term scales and mechanistic controls of surface seawater fugacity of CO_2 (fCO_2^{sw}) within contrasting physical-chemical regimes (Keeling, 1968; Lefèvre, 1997) in spring and autumn. The diversity of oceanographic provinces sampled during the FICARAM cruises were marked and varied from highly productive areas located in upwelling systems to oligotrophic intertropical gyres. The cruise tracks also covered large areas in the North and South Atlantic Oceans, which are known to behave as important sinks of atmospheric CO_2 at present (Takahashi et al., 2009). The fluctuation in the major modes of climate variability, in particular, North Atlantic Oscillation (NAO), El Niño – Southern Oscillation (ENSO) and Southern Annular Mode (SAM) have been linked to observed anomalies of fCO_2 (Patra et al., 2005; Lovendruski et al., 2007; Borges et al., 2008) and other biochemical variables (Enfield and Mayer, 1997; Labat et al., 2005) in the Atlantic Ocean. In this sense, particular changes in the spatial fCO_2^{sw} patterns of the North Atlantic Ocean were strongly related to the NAO index during the FICARAM period (Schuster and Watson, 2007; Schuster et al., 2009; Ullman et al., 2009)

In this paper, we summarize the underway fCO_2^{sw} measurements along a meridional transect of the Atlantic Ocean during the spring and autumn seasons since 2000 through 2008. The aim of this work is to characterize the differences of air-sea CO_2 fluxes and their biogeochemical forcing, and analyze the long-term trends observed in these variables during the FICARAM cruises.

2 Dataset and methods

2.1 The FICARAM cruises

The fourteen FICARAM cruises were conducted on board the research vessels *B/O Hespérides* and *B/O Las Palmas* beginning in October 2000 to November 2008 (Table 1). The cruise tracks covered approximately the same transit between the southern Spanish coasts and the Southern Ocean (Fig. 1). The heading of the courses was always southwards during the boreal autumn and northwards in boreal springs. The cruises were conducted as part of the Antarctic research program for maintenance and supplying the Spanish Antarctic

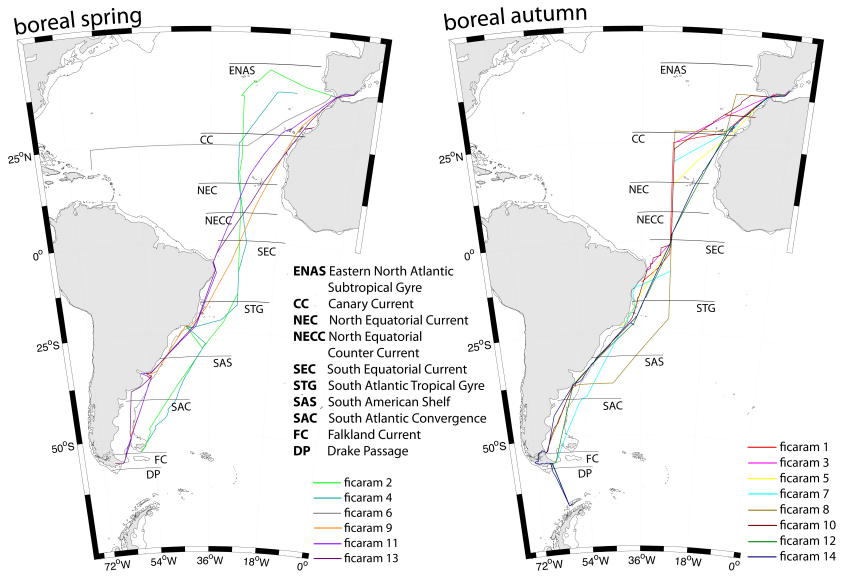

Fig. 1. Map showing the ship tracks and biogeochemical provinces selected for the FICARAM cruises. Left panel gives boreal spring tracks and right panel the boreal autumn ones.

bases Gabriel de Castilla and Juan Carlos I, located in the Deception and Livingston Islands, respectively.

The FICARAM cruises were principally conducted in the Eastern North and Western South Atlantic basins. Initially, cruises were intended to sail as close as possible to meridian 28^{o}W while underway, but this was normally subject to ship-time availability. This practice ceased after the FICARAM 9 cruise, when the vessels started operating as ships of opportunity and sailed directly from departure to arrival ports. Nevertheless, sufficient cruises were conducted to study the meridional variability of fCO_2^{sw}.

2.2 Equipment installation

The underway measurements of sea-surface and atmospheric molar fractions of CO_2 (xCO_2^{sw} and xCO_2^{atm}, respectively) were performed with a GASPAR apparatus, an autonomous device assembled at Instituto de Investigacións Mariñas (IIM-CSIC, Vigo-Spain). The device configuration was based on a previous setup developed by researchers at the Institut für Meereskunde (Kiel – Germany; Körtzinger et al., 1996). The analytical principle is based on the equilibration of atmospheric air with the seawater sample under analysis.

There are several existing techniques available for achieving equilibration between a carrier gas phase and a seawater sample. The air – sea equilibrator system combines the advantages of a laminar flow system (Poisson et al., 1993) with a bubble-type system (Takahashi, 1961). The bubble equilibrator consists of a 1.5 L volume chamber through which surface seawater was being constantly pumped from 3 m under the waterline into the ship's hull through the ships non-toxic seawater supply system. The laminar flow equilibrator consisted of a 30 cm high glass column with two concentric cylinders to provide thermal insulation. The sampled seawater flowed at a rate of 1.5–2 L min^{-1} that was inputted from the top of the equilibrator's water chamber. A fixed volume of air was constantly recirculated through this system (0.8 L min^{-1}) in order to favour rapid equilibration with the seawater phase. The system was vented to the atmosphere through an air ballast bottle flushed by an external airline stream which avoided enriched CO_2 air inputs from the laboratory.

A thermosalinograph (SBE-45-MicroTSG) was connected to the same uncontaminated seawater supply. This apparatus recorded underway surface temperature (SST) and salinity (SSS) during the cruises conducted on board *B/O Las Palmas*. When on board the *B/O Hespérides*, these data were gathered via the vessel-mounted oceanographic data acquisition system.

The molar fractions of CO_2 and H_2O were measured with a non-dispersive infrared Li-COR analyser (model 6262) that is characterized by a stable drift over the long term. This precision experimental procedure is well documented and serves to determine the partial pressure of CO_2 (pCO_2) in an air-flushed equilibrator (Takahashi, 1961). The Li-COR instrument utilises a reference channel (apart from the measuring channel) where a dry CO_2-free gas recirculates at a rate of 0.2 L min^{-1}. Two standards were used through this channel, namely: a CO_2-free air and a CO_2 standard gas of known concentration (375 ppm) certified by Instituto Meteorológico Nacional de Izaña (Canary Islands, Spain).

Gas mixtures were introduced in the Li-COR analyser via miniature solenoid valves, which were used to switch between gas inputs from various sources: atmospheric air,

equilibrated air from the samples and the gas standards. A typical analytical cycle consisted of a calibration phase, which involved 20 measurements of each of the two gas standards. Immediately after calibration, the apparatus performs 24 uninterrupted sample measurements for about an hour, out of which 55 min were devoted to seawater equilibrated sample measurements and 5 min for atmospheric air records. The surface seawater observations were initially estimated with a 1-min frequency and averaged every 5-min cycle.

Remotely sensed chlorophyll *a* (chl *a*) was included in the presented FICARAM dataset as a proxy of the photosynthetic activity. Weekly fields of chl *a*, with a spatial resolution of 9 km^2 were remotely recorded by Sea-viewing Wide Field-of-view Sensor (SeaWIFS) Level 3 (Hooker et al., 1992) and downloaded from http://oceancolor.gsfc.nasa.gov/. The selected satellite records of chl *a* do not have an exact spatiotemporal match with ship measurements. Selection criteria for the choice of pixels consisted in considering only SeaWIFS measurements taken within ± 4 days (orbital over-passing) of the ship measurement date and found within ± 6.3 km off the track of the cruise.

2.3 Estimation of air and sea fCO_2 and air-sea CO_2 exchanges

The xCO_2^{atm} values were linearly interpolated versus latitude, using monthly measurements from selected meteorological stations of the NOAA/ESRL Global Monitoring Division located close to ship tracks (Fig. 1), namely: Mace Head (Ireland, 53.33° N), Azores (Portugal, 38.77° N), Izaña (Spain, 28.3° N), Ascension (UK, 7.92° S), Arembepe (Brazil, 12.77° S), Tierra de Fuego (Argentina, 54.87° S) and Palmer Station (US, 64.92° S). This dataset was preferred to in situ xCO_2^{atm} data due to the lack of these records during the last five cruises on board the B/O Las Palmas. For consistency, measurements from the NOAA/ESRL were used in all cases. The record gaps in the time-series from these stations were completed fitting the in situ xCO_2^{atm} recordings to a theoretical curve combining a seasonal cycle trend with the annual and semi-annual harmonics (Padin et al., 2007). The final xCO_2^{atm} dataset was then converted to pCO_2^{atm} (Eq. 1) considering the atmospheric pressure (p^{atm}) and the partial pressure of water vapour (pH_2O), which was calculated from in situ SST readings (Tis; Cooper et al., 1998) (Eq. 2). The pCO_2^{atm} values were then converted to fCO_2^{atm} assuming a decrease of 0.3% from the pCO_2^{atm} value (Weiss, 1974).

$$pCO_2^{atm} = xCO_2^{atm}(p^{atm} - pH_2O) \quad (1)$$

$$pH_2O = 0.981\exp(14.32602 - (5306.83/(273.15 + T_{is}))) \quad (2)$$

The measured xCO_2^{sw} data was converted to fCO_2^{sw} referenced to saturated water vapour pressure using in situ p^{atm} readings. The fCO_2^{sw} values were then corrected for the seawater temperature drift that occurs while the sample travels from the hull's inlet into the equilibration chamber. This temperature shift was usually $< 1°C$. The temperature tracking was done with platinum resistance thermometers and then applying the empirical equation proposed by Takahashi et al. 1993; $\delta \ln pCO_2/\delta T = 0.04231°C^{-1}$).

$$FCO_2 = kS\Delta fCO_2 \quad (3)$$

The FCO_2 (mol $m^{-2}\,yr^{-1}$) was calculated applying Eq. 3, where "*S*" stands for the solubility of CO_2 in seawater (Weiss et al., 1974), "*k*" is the CO_2 transfer velocity (Wanninkhof, 1992) and ΔfCO_2 (μatm) is the air-sea fCO_2 gradient (i.e., $fCO_2^{sw} - fCO_2^{atm}$). The coefficient "*k*" was computed using daily wind speed (WS) data obtained from NCEP-DOE AMIP-II Reanalysis (Kalnay et al., 1996). Data was accessed via the website of the NOAA-CIRES Climate Diagnostics Center, Boulder, Co, USA (http://www.cdc.noaa.gov/).

2.4 Biogeochemical oceanographic provinces

The study of the meridional distribution of the fCO_2^{sw} measurements in the Atlantic Ocean (excluding the Mediterranean basin) focuses on selected biogeochemical provinces established after Longhurst et al. (1995) and Hooker et al. (2000). Different sections of the FICARAM tracks were allocated in the appropriate following ten regions according to average boundaries established from SST–SSS relationships (Fig. 1):

- (a) *Eastern North Atlantic Subtropical Gyre* (ENAS; 39° N–27° N) dominated by the Azores Current (Ríos et al., 1992) and comprising the northeast component of the North Atlantic Subtropical Gyre.

- (b) The *Canary Current* (CC; 27° N–16° N) is also part of the northern subtropical gyre with a moderate flow characterised by a salinity maximum that demarcates the beginning of the tropics. A coastal upwelling with a weak seasonality was located in the West African continental margin at these latitudes (Mittelstaedt, 1991).

- (c) The *North Equatorial Current* (NEC; 16° N–8° N) region is located amidst the zonal currents of the Equatorial Atlantic. This latitudinal band includes the Guinea Dome province (12° N–8° N), characterized by seasonal upwelling events that occur from December through May (Barton et al., 2001). At these latitudes, the chl *a* signal extends from the coast to the open oceans during the upwelling peak from February to May (Aristegui et al., 2009). During the summer this offshore growth of phytoplankton community abruptly drops.

- (d) The *North Equatorial Counter Current* province (NECC; 8° N–1° N) features a maximum flow from the easterly current during the Boreal Autumn that fades away during the winter and early spring (Richardson

and Reverdin, 1987). The seasonal changes in the location of the NECC were associated with the position of the InterTropical Convergence Zone. This province is also characterized by a band of low-density waters from the Amazon River with a core at 4° N–5° N (Müller-Karger et al., 1988) with SST values of ∼25 °C and a SSS<35 (Emery & Dewar, 1982).

– (e) The *South Equatorial Current* province (SEC; 1° N–15° S) features a seasonal forcing with a maximum westward flow during the austral winter in the vicinity of the Equator. The South Equatorial Counter Current was weakly present between 7° S–9° S.

– (f) The *South Atlantic Tropical Gyre* province (STG; 15° S–31° S) exhibits relatively stable thermohaline properties with a gradual decrease of its SST and SSS values. An important poleward component of the Brazil Current that ran along the South American continental shelf is also present in this region.

– (g) The *South American Shelf* province (SAS; 31° S–40° S) is dominated by the Brazil Current as well, which extended southward as far as 44° S, in conjunction with a strong influence from the Plata river.

– (h) The *South Atlantic Convergence* zone (SAC; 40° S–51° S) is a frontal area where the northward Falkland and southward Brazil currents converge. This characteristic generates high temperature gradients and large heterogeneity in the concentration fields of several chemical properties.

– (i) The *Falkland Current* (FC; 51° S–56° S) is a northward looping excursion of the Circumpolar Current that forms a jet of SST and SSS under 10 °C and 34.3, respectively (Bianchi et al., 1993).

– (j) The Drake Passage region, (DP; 56–66° S) extends from the southernmost tip of South America (56° S) to the northern tip of the Antarctic Peninsula (62° S). It is dominated by a racing eastward flow of the Antarctic Circumpolar Current. The Southern Ocean is characterized by a latitudinal succession of circumpolar frontal structures such as the Subantarctic Front, the Polar Front and the Continental Water Boundary.

A depth of 200 m was chosen as a boundary to separate ocean areas from shelf areas (Fig. 1). The CO_2 source-sink behaviour changes in the continental shelf with respect to deeper waters were also considered: while the distal shelf normally behaves as a CO_2 sink, the proximal shelf is essentially influenced by continental inputs and non-stratified conditions that favour the outgasing of CO_2 to the atmosphere (Thomas et al., 2004; Padin et al., 2007; Chen and Borges, 2009). Consequently, surface coastal waters (<50 m) that corresponded mainly to harbour areas were excluded from the database. The ETOPO2v2 (USDC, NOAA, NGDC 2006) bathymetry was used for merging depth records using two-dimensional linear interpolation functions of every measurement. After applying all of these selection criteria filters, a final FICARAM dataset comprising 67845 observations was put together.

3 Results

3.1 Overiew of the spatial variability of the FICARAM dataset

Figures 2 and 3 graphically depict the meridional distribution of SST, SSS, ΔfCO_2 and FCO_2 measurements along the Atlantic Ocean (Fig. 1) during the spring and autumn seasons. Table 2 shows the mean values and the standard deviation of these variables including WS and chl *a* within the separated regions.

The meridional distribution of SST showed a clear inter-hemispheric symmetry that resulted from meridional differences in the Earth's radiation balance. Subtropical latitudes were characterized by spring–autumn differences of SST: during the boreal autumn, waters were warmer in the northern than in the southern hemisphere while during boreal spring, waters were warmer in the southern hemisphere compared to the Northern Hemisphere (Fig. 2a, c). The observed SST changes were negligible in the equatorial region between spring and autumn (Table 2). The spatial variability of the SSS measurements also showed an inter-hemispheric symmetry that disappeared in the Southern regions (Fig. 2b, d). Contrary to the SST distribution, the intense intertropical (23.4° S–23.4° N) precipitation rates reduce SSS values in the equatorial waters (Fig. 2b, d; Table 2) causing a clear minimum and reversing the direct SST–SSS relationship observed in the subtropical regions.

ΔfCO_2 variability in the Northern North Atlantic (Fig. 3b, d) loosely followed the seasonal SST changes. Lower values of fCO_2^{sw} compared to fCO_2^{atm} prevailed in the boreal spring (Table 2) while high fCO_2^{sw} values, which resulted in CO_2 oversaturation of the surface waters occurred during the boreal autumn. With the exception of the coastal regions, highest and lowest ΔfCO_2 values along the Atlantic Ocean were located in the SEC region and in the Patagonian Sea, respectively (Fig. 3b, d). FCO_2 estimations computed from ΔfCO_2 of the FICARAM dataset reproduced well the known behaviour of the tropical regions as sources of atmospheric CO_2 and the seasonally shifting role of the subtropical ocean waters (Table 2). The Patagonian Sea permanently acted as sink of atmospheric CO_2 reaching the strongest CO_2 uptake along the FICARAM cruises in autumn (Fig. 3a, c; Table 2). Shelf waters sampled along the coasts of Africa and South America generally followed the behaviour of the adjacent ocean waters emphasizing the observed changes between spring and autumn with minor exceptions located in STG and FC regions (Table 2).

Table 2. Statistics for the selected provinces on the different boreal seasons (spring; autumn) and areas (shelf; ocean): Mean and standard deviation ($\mu \pm \sigma$) of SST, SSS, chl *a*, ΔfCO_2, WS, FCO_2.

Region	Boreal Season	Area	SST °C	SSS	chl *a* mg m^{-3}	ΔfCO_2 µatm	WS m s^{-1}	FCO_2 mol m^{-2} yr^{-1}
ENAS 39–27° N	*spring*	*shelf*	*18.1 ± 0.2*	*36.4 ± 0.0*	*0.04 ± 0.00*	*−43 ± 1*	*6.9 ± 0.7*	*−2.0 ± 0.0*
		ocean	*18.6 ± 0.9*	*36.6 ± 0.2*	*0.11 ± 0.07*	*−34 ± 12*	*7.4 ± 2.5*	*−1.8 ± 1.2*
	autumn	shelf	22.0 ± 0.6	36.5 ± 0.2	0.15 ± 0.06	2 ± 11	5.3 ± 4.2	0.3 ± 0.6
		ocean	22.9 ± 1.1	36.7 ± 0.2	0.14 ± 0.12	9 ± 13	5.2 ± 2.7	0.2 ± 0.4
CC 27–16° N	*spring*	*shelf*	*18.4 ± 0.2*	*36.3 ± 0.1*	*0.11 ± 0.01*		*6.8 ± 1.0*	
		ocean	*21.3 ± 1.1*	*36.6 ± 0.5*	*0.13 ± 0.09*	*−19 ± 13*	*8.9 ± 1.4*	*−1.4 ± 1.0*
	autumn	ocean	25.3 ± 1.5	36.7 ± 0.4	0.12 ± 0.06	16 ± 13	6.6 ± 2.6	0.6 ± 0.5
NEC 16–8° N	*spring*	ocean	*24.9 ± 1.3*	*35.9 ± 0.2*	*0.13 ± 0.07*	*−17 ± 10*	*7.6 ± 1.8*	*−0.7 ± 0.4*
	autumn		28.1 ± 0.6	35.7 ± 0.4	0.12 ± 0.06	2 ± 14	6.1 ± 2.0	0.0 ± 0.5
NECC 8–1° N	*spring*	ocean	*28.1 ± 0.5*	*35.6 ± 0.3*	*0.14 ± 0.08*	*1 ± 16*	*5.5 ± 1.7*	*0.1 ± 0.4*
	autumn		28.2 ± 0.6	35.1 ± 0.5	0.11 ± 0.04	3 ± 13	4.5 ± 1.8	0.1 ± 0.3
SEC 1° N–15° S	*spring*	*shelf*	*29.1 ± 0.3*	*37.0 ± 0.2*	*0.17 ± 0.01*		*2.0 ± 0.2*	
		ocean	*28.7 ± 0.3*	*36.3 ± 0.6*	*0.18 ± 0.08*	*30 ± 11*	*4.2 ± 2.0*	*0.7 ± 0.5*
	autumn	shelf	27.1 ± 0.3	36.5 ± 0.2	0.16 ± 0.04	34 ± 8	7.1 ± 1.1	1.6 ± 0.6
		ocean	26.8 ± 0.5	36.3 ± 0.3	0.14 ± 0.05	24 ± 12	7.0 ± 1.6	1.0 ± 0.7
STG 15–31° S	*spring*	*shelf*	*26.3 ± 1.5*	*36.4 ± 0.5*	*0.15 ± 0.05*	*17 ± 17*	*5.0 ± 1.5*	*0.4 ± 0.4*
		ocean	*27.4 ± 1.0*	*36.9 ± 0.3*	*0.17 ± 0.06*	*21 ± 14*	*5.8 ± 1.9*	*0.6 ± 0.6*
	autumn	shelf	23.8 ± 1.5	36.5 ± 0.5	0.13 ± 0.02	14 ± 9	8.6 ± 3.2	0.5 ± 0.7
		ocean	23.9 ± 1.7	36.8 ± 0.4	0.17 ± 0.07	−5 ± 17	6.9 ± 1.7	−0.2 ± 0.7
SAS 31–40° S	*spring*	*shelf*	*22.1 ± 2.0*	*33.2 ± 2.2*	*0.28 ± 0.16*	*−19 ± 27*	*5.4 ± 2.7*	*−0.7 ± 1.3*
		ocean	*20.7 ± 4.1*	*35.0 ± 1.1*	*0.24 ± 0.10*	*−28 ± 30*	*6.1 ± 2.8*	*−0.9 ± 1.5*
	autumn	shelf	14.9 ± 2.5	32.6 ± 1.1	0.18 ± 0.09	−67 ± 37	7.4 ± 2.2	−3.2 ± 2.7
		ocean	17.8 ± 1.8	35.6 ± 0.5	0.11 ± 0.04	−41 ± 16	7.1 ± 3.1	−2.2 ± 2.1
SAC 40–51° S	*spring*	*shelf*	*10.4 ± 0.6*	*33.6 ± 0.1*	*0.26 ± 0.05*	*−42 ± 9*	*9.0 ± 1.1*	*−3.2 ± 1.1*
		ocean	*11.9 ± 2.2*	*34.0 ± 0.2*	*0.26 ± 0.10*	*−39 ± 16*	*7.4 ± 3.8*	*−1.9 ± 2.1*
	autumn	shelf	9.5 ± 2.1	33.4 ± 0.3	0.11 ± 0.03	−70 ± 42	8.2 ± 3.4	−4.1 ± 4.0
		ocean	9.3 ± 1.4	33.8 ± 0.1	0.15 ± 0.06	−57 ± 26	9.9 ± 3.1	−5.4 ± 3.6
FC 51–56° S	*spring*	*shelf*	*9.2 ± 0.6*	*33.3 ± 0.3*	*0.40 ± 0.15*	*−7 ± 23*	*10.8 ± 4.8*	*−0.7 ± 2.8*
		ocean	*8.8 ± 0.5*	*33.6 ± 0.2*	*0.43 ± 0.22*	*1 ± 26*	*10.6 ± 5.3*	*1.2 ± 2.5*
	autumn	shelf	6.6 ± 0.8	32.9 ± 0.5	0.09 ± 0.04	−15 ± 32	10.4 ± 3.0	−1.4 ± 3.2
		ocean	6.8 ± 1.1	33.6 ± 0.4	0.08 ± 0.02	−50 ± 40	9.7 ± 3.5	−2.8 ± 2.5
DP 56–66° S	autumn	shelf	−0.8 ± 0.7	34.1 ± 0.1	0.14 ± 0.05	8 ± 14	3.9 ± 1.6	0.1 ± 0.3
		ocean	1.3 ± 2.3	33.8 ± 0.2	0.10 ± 003	−20 ± 11	6.8 ± 3.0	−1.1 ± 0.9

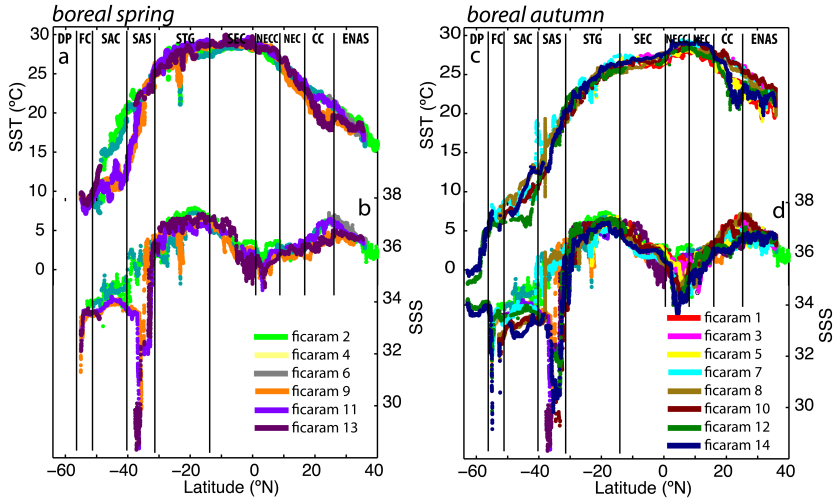

Fig. 2. Latitudinal distributions during boreal springs **(a, b)** and boreal autumns **(c, d)** of SST and SSS as measured in the FICARAM cruises.

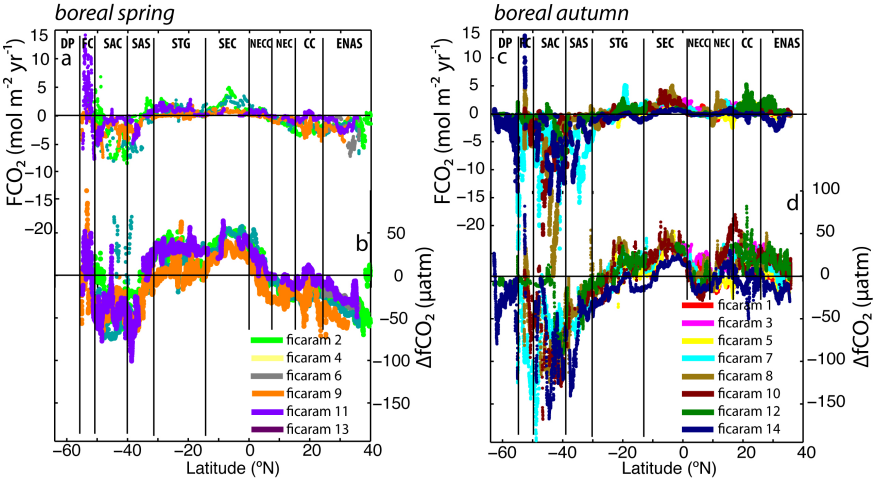

Fig. 3. Latitudinal distributions during boreal springs **(a, b)** and boreal autumns **(c, d)** of FCO_2 and ΔfCO_2 as measured in the FICARAM cruises.

3.2 Observed distribution of biogeochemical variables in the Atlantic provinces

Eastern North Atlantic Subtropical Gyre (ENAS): Equatorward warming and modest increase in SSS characterized the surface waters of the ENAS province during spring and autumn seasons (Fig. 2). The seasonal variability of the SST observations that reached 4.3 °C in the ocean waters and was the largest observed in the Atlantic Ocean (Table 2). On the contrary, SSS measurements in April and autumn closely agreed to an average value of 36.6 showing a change lower than 0.1 (Table 2).

Ocean waters of the ENAS region were considerably undersaturated during spring in relation to the atmosphere (-34 ± 12 µatm) and sligthly oversaturated in autumn (9 ± 13 µatm). This spring–autumn shift of ΔfCO_2 of 43 µatm was the highest observed among the regions of the North Atlantic Ocean. Hence oceanic waters acted as a considerable sink of atmospheric CO_2 of $-1.8 \pm 1.2\,mol\,m^{-2}\,yr^{-1}$ in April and a small CO_2 source of $0.2 \pm 0.4\,mol\,m^{-2}\,yr^{-1}$ in autumn. The FCO_2 exchange in coastal waters essentially mirrored those observed in open ocean waters with a slight intensification. So, the surface waters of the shelf region showed the largest seasonal span in the FCO_2 ranging from $-2.0 \pm 0.0\,mol\,m^{-2}\,yr^{-1}$ and $0.3 \pm 0.6\,mol\,m^{-2}\,yr^{-1}$ in spring and autumn (Table 2), respectively.

The *Canary Current* (CC): The dataset collected in the CC region also revealed the increase of SST and ΔfCO_2 to the south, as was observed in the ENAS region. The surface waters were appreciably warmer than surface waters found in the ENAS region by 2.7 °C and 2.4 °C during spring and autumn, respectively. On the contrary a SSS decrease from a maximum value located at around 27° N was also observed during both seasons in parallel with the equatorward warming. Similarly to the surface waters of the ENAS region, the CC region acted as a CO_2 sink (-1.4 ± 1.0 mol m^{-2} yr^{-1}) in spring and a modest CO_2 source of 0.6 ± 0.5 mol m^{-2} yr^{-1} in autumn.

The effects of the upwelling events were observed in the cruises conducted closer to the coast at these latitudes. As a result, ΔfCO_2 values of up to 50 µatm during autumn (Fig. 3d) were found at around 20° N associated with the cold upwelled water (Fig. 2b). In the same region, an intense CO_2 undersaturation exceeding -50 µatm was also found along the Mauritanian coast (Fig. 3d) coincident with an intense photosynthetic activity. Remotely sensed chl *a* observations revealed values of 1.3 mg m^{-3} (data not shown).

The *North Equatorial Current* (NEC): The surface waters of the NEC region supported the equatorward warming and the decrease of SSS observed in the CC region. On the other hand, ΔfCO_2 measurements (Fig. 2) did not follow the meridional distribution. Surface waters during spring showed an underaturation of -17 ± 10 µatm (Table 2) in spring and a value of 2 ± 14 µatm in autumn pointing out equilibrium CO_2 situation with the atmosphere of these waters after summer.

The *North Equatorial Counter Current* province (NECC): North of the equator, a distinct wide band of low SSS values characterized the surface waters of the NECC province. These less saline waters of the ocean waters reached the lowest mean value of 35.1 ± 0.5 of the North Hemisphere in March–April showing an outstanding SSS shift of 0.5 from spring to autumn. Conversely the seasonal variability of SST that reached the highest value in boreal autumn season of 28.2 ± 0.6 °C was practically absent and the spring–autumn range of ΔfCO_2 and fCO_2 also showed minimal variability. The NECC waters acted as small CO_2 sources to the atmosphere in both seasons (Table 2) with mean values of 0.1 mol m^{-2} yr^{-1} estimated from ΔfCO_2 of 1 ± 16 and 3 ± 13 µatm in spring and autumn, respectively.

The *South Equatorial Current* (SEC): Average SST values of 29.1 ± 0.3 and 28.7 ± 0.3 °C in spring characterised the shelf and ocean areas of the SEC as having the warmest waters along FICARAM cruises (Table 2). The ocean waters also showed the highest CO_2 supersaturation in spring and autumn with ΔfCO_2 values of 30 ± 11 and 24 ± 12 µatm, respectively. Despite these observations, a stronger CO_2 outgassing of 1.0 ± 0.7 mol m^{-2} yr^{-1} was estimated in autumn because of the relatively higher wind speeds of 7.0 ± 1.6 m s^{-1}. In any case, SEC waters were the most important sources of CO_2 to the atmosphere in the current study.

The *South Atlantic Tropical Gyre* province (STG): The subtropical waters of the South Hemisphere showed notable changes from spring to autumn that were opposite to those of the North Atlantic. The distribution of SST and SSS showed a direct correlation. Both variables showed a poleward declination that reflects the heat loss of waters and the influence of continental inputs (Fig. 2). This pattern was closely repeated in the ΔfCO_2 distribution (Fig. 3b, d). Mean ΔfCO_2 values of the ocean waters were 21 ± 14 µatm in March–April and -5 ± 17 µatm in October-November and so, they acted as a source of 0.6 ± 0.6 mol m^{-2} yr^{-1} in spring and as a small sink of -0.2 ± 0.7 mol m^{-2} yr^{-1} in autumn (Table 2). The distal shelf of Brazil coast at these latitudes was a slight CO_2 source in both seasons of 0.4 ± 0.4 and 0.5 ± 0.7 mol m^{-2} yr^{-1} in the period March–April and October–November, respectively (Table 2).

The *South American Shelf* province (SAS): The recordings in this region were mostly confined to the South American continental shelf that allowed the clear influence of inputs from the River Plate. The fluvial discharges decreased SSS to 32.6 ± 1.1 in November which was the lowest value along the Atlantic Ocean. The shelf and ocean waters of the SAS region were strongly undersaturated and acted as a strong CO_2 sink during both seasons (Fig. 3). The CO_2 undersaturation was especially intense over the shelf-break in November reaching ΔfCO_2 values lower than -190 µatm (Fig. 2g) and an average CO_2 absorption of -3.2 ± 2.7 mol m^{-2} yr^{-1} (Table 2). During the same month, oceanic waters showed a CO_2 sink with a strength of -2.2 ± 2.1 mol m^{-2} yr^{-1}. The CO_2 uptake of the surface waters in March showed SST values up to 20 °C was -0.9 ± 1.5 mol m^{-2} yr^{-1} and -0.7 mol m^{-2} yr^{-1} in the ocean and coastal waters, respectively (Table 2).

The *South American Convergence* zone (SAC): The confluence of the warm and saline Brazil Current and the cold and less saline Falkland Current at these latitudes caused relatively high spatial heterogeneity of SSS and SST distributions (Fig. 2). This region showed relatively strong changes in the SST and SSS distribution that reached ∼6 °C and ∼2 during FICARAM 7 (Fig. 2). In spite of this variability, these waters acted as very strong sink of atmospheric CO_2 during both seasons as found in the SAS region. The strongest undersaturation of the ocean waters of -57 ± 26 µatm in November modulated by an intense WS of 9.9 ± 3.1 m s^{-1} resulted in fCO_2 value of -5.4 ± 3.6 mol m^{-2} yr^{-1} (Table 2). This was the highest CO_2 uptake estimated along the Atlantic Ocean for this study (Fig. 3c).

The *Falkland Current* (FC): Oceanic waters of the FC region in March were sligthly supersaturated in CO_2 by 1 ± 26 µatm in spite of high chl *a* value of 0.43 ± 0.22 mg m^{-3}. The ΔfCO_2 values close to the air-sea equilibrium observed through the "furious fifties" of the Southern Ocean with WS up to 10 m s^{-1} resulted in CO_2

outgassing of $1.2 \pm 2.5\,\mathrm{mol\,m^{-2}\,yr^{-1}}$ (Table 2). In November, the same area reversed its role becoming a large CO_2 sink of $-2.8 \pm 2.5\,\mathrm{mol\,m^{-2}\,yr^{-1}}$. Shelf waters did not exhibit the same seasonal shift and acted as a sink of CO_2 during both seasons (Table 2). The CO_2 uptake of these waters in November was estimated at $-1.4 \pm 3.2\,\mathrm{mol\,m^{-2}\,yr^{-1}}$ during autumn in association with low SSS values of 32.9 ± 0.5 (Fig. 2d; Table 2). More saline waters (33.3 ± 3) on the shelf area were found in March showing a CO_2 absorption of $-0.7 \pm 2.8\,\mathrm{mol\,m^{-2}\,yr^{-1}}$.

The *Drake Passage* region (DP): These waters of the Southern Ocean were only sampled in November 2007 and 2008. The meridional distribution in this branch of the Southern Ocean showed a marked thermohaline distribution with two strong gradients at ∼57° S and ∼58.7° S. These features represent the known zonation of Antarctic waters, that is, the Subantarctic Front and the Polar Front, respectively, delimiting the Antarctic Circumpolar Current. This pattern was narrowly repeated in the four cruises during both autumns (Fig. 2). In the shelf waters of the Livingston Island, SST had a mean value of $0.8 \pm 0.7\,^{\circ}\mathrm{C}$ (Table 2) which was the lowest one along the Atlantic Ocean. To the south of the Polar Front, SSS showed a clear onshore increase (Fig. 2d).

Opposite values in the CO_2 saturation in relation to the atmosphere were found in the shelf and ocean waters. Ocean waters were undersaturated with values of $-10 \pm 4\,\mu\mathrm{atm}$ in November 2007 and $-21 \pm 21\,\mu\mathrm{atm}$ during November 2008. The stronger undersaturation of 2008 was characterized by a southward intensification along the Drake Passage reaching a minimum value around $-80\,\mu\mathrm{atm}$ at ∼62° S. Surface waters over the distal shelf showed an average oversaturation of $8 \pm 14\,\mu\mathrm{atm}$ (Fig. 3d; Table 2) that followed an onshore increase similar to the SSS distribution. Therefore ocean waters of the Southern Ocean along the Drake Passage acted as a sink of $-1.1 \pm 0.9\,\mathrm{mol\,m^{-2}\,yr^{-1}}$ while coastal waters released CO_2 to the atmosphere with a mean rate of $0.1 \pm 0.3\,\mathrm{mol\,m^{-2}\,yr^{-1}}$ during the successive November (Table 2).

3.3 Long-term trend in biogeochemical variables during the FICARAM cruises from 2000 to 2008

The long-term trends from years 2000 to 2008 of the variables measured and estimated from the database gathered during the FICARAM cruises were studied from the interannual changes in each province (Fig. 4). These temporal changes were only evaluated in oceanic waters in order to avoid the high susceptibility of coastal waters to anthropogenic and climatic forcing (Wolf-Gladrow et al., 1999; Anderson and Mackenzie 2004; Bakun et al., 2010). In addition data from the Western basin of the North Atlantic Ocean that were only sampled during spring 2007 (Fig. 1) were excluded due to the differences with the Eastern basin (Lüger et al., 2004). Furthermore we assume the influence of the longitudinal variability of the FICARAM tracks on the long-term trends was almost null. The mean values of every variable were linearly fitted to identify significant decadal trends ($p < 0.05$) during the successive springs and autumns. These interannual trends should only be taken into account as year-to-year trends of these seasons due to the seasonal variability of the long-term variability (Lefevre et al., 2004; Padin et al., 2009).

The provinces of the North Atlantic Ocean (Fig. 4a, b and c) showed an appreciable but not significant warming of the surface waters during the cruises of spring and autumn seasons. In addition to the observed long-term trend of SST, the subtropical surface waters roughly pointed out a slight increase of ΔfCO_2 and a weakening of the oceanic uptake of CO_2 (Fig. 4a, b, and c) as well. Other variables with a direct influence on the air-sea CO_2 exchange showed highly statistically significant changes in the subtropical waters. Thus, a declination of the WS of $-0.30 \pm 0.07\,\mathrm{m\,s^{-1}\,yr^{-1}}$ was found in the CC province during the successive spring cruises (Fig. 4b) that was also accompanied by a minor decrease in SSS. The spring chl *a* distribution also showed a significant interannual trend of $-0.3 \pm 0.1\,\mathrm{mg\,m^{-3}\,yr^{-1}}$ (Fig. 4c) in the NEC province.

Significant interannual changes were particularly pronounced in the equatorial regions. The NECC region showed a sustained decrease of $-0.16 \pm 0.01\,\mathrm{yr^{-1}}$ in SSS during the autumn season (Fig. 4d). Besides the observed SSS drop, an increase of the undersaturation in CO_2 of $-3.5 \pm 0.9\,\mu\mathrm{atm\,yr^{-1}}$ and of the ocean CO_2 uptake of $-0.09 \pm 0.03\,\mathrm{mol\,m^{-2}\,yr^{-2}}$ characterized the NECC province. To the south of the equator, the tropical waters of SEC province showed a significant warming of $0.11 \pm 0.03\,^{\circ}\mathrm{C\,yr^{-1}}$ during the successive autumn cruises that was the only interannual SST change found along the Atlantic Ocean. Apart from this significant warming, the interannual WS variation also showed a noteworthy decrease of $-0.58 \pm 0.14\,\mathrm{m\,s^{-1}\,yr^{-1}}$ during the same season. It is noticeable that, in general terms, the trend observed in ΔfCO_2 and FCO_2 in the equatorial regions was opposite to the ones found in the subtropical latitudes.

On the Patagonian Sea, the surface waters of the SAS and SAC regions during consecutive spring seasons were also influenced by a drop in WS of $-0.50 \pm 0.11\,\mathrm{m\,s^{-1}\,yr^{-1}}$ and of $-1.24 \pm 0.26\,\mathrm{m\,s^{-1}\,yr^{-1}}$, respectively (Fig. 4g, h).

3.4 Analysis of the biogeochemical forcing on the fCO_2^{sw} variability

The correlations between fCO_2^{sw} and the ancillary parameters in the ocean waters were explored to identify the processes controlling fCO_2^{sw} variability during the FICARAM cruises. These fCO_2^{sw} measurements were modelled with an empirical algorithm according to biochemical forcing (Olsen et al., 2004; Ono et al., 2004; Wanninkhof et al., 2007; Lueger et al., 2008; Padin et al., 2008). Spring and autumn measurements were separated as in the study of long-term

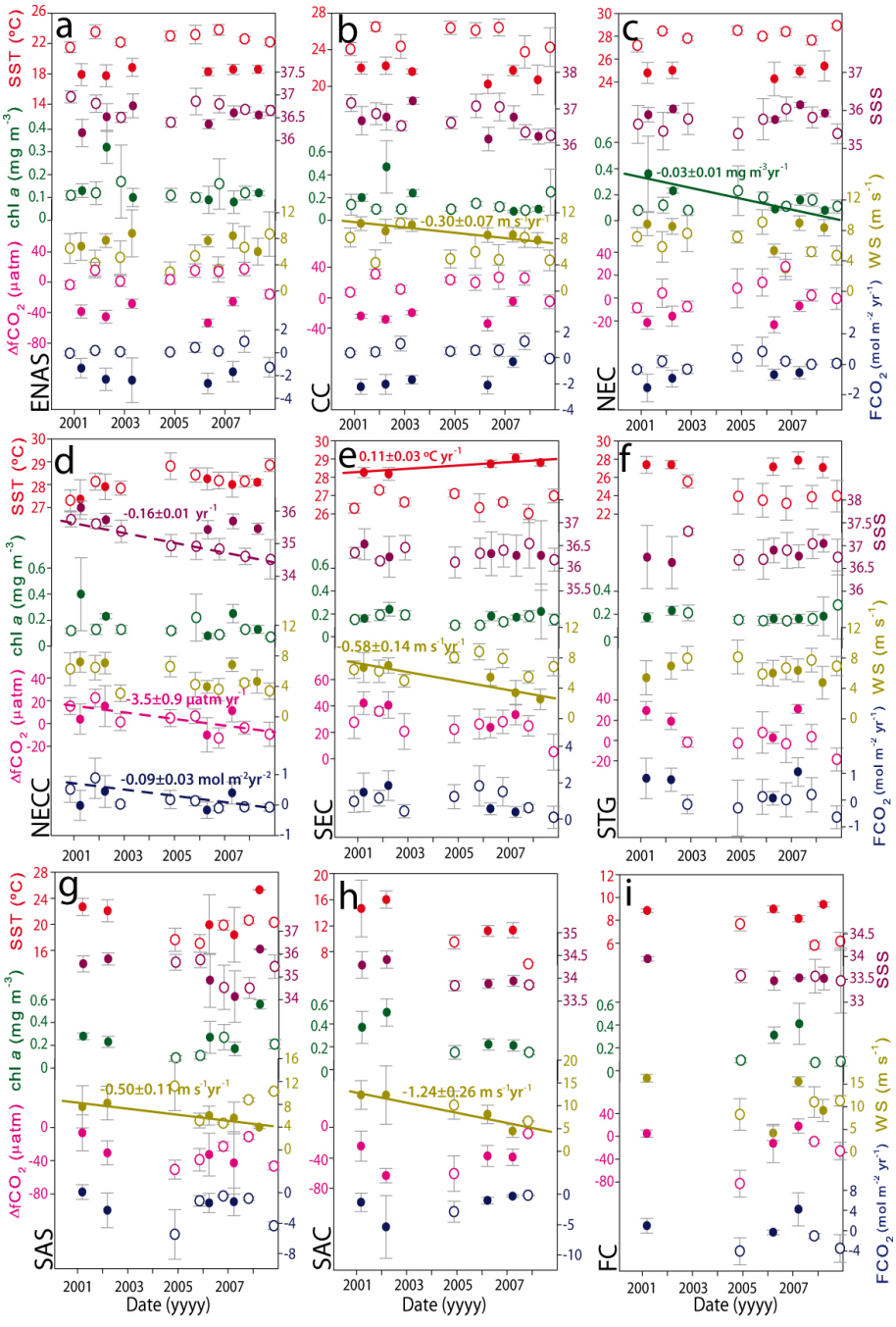

Fig. 4. Temporal variation of the averaged SST, SSS, chl *a*, WS, ΔfCO_2 and FCO_2 cruise (error bars stand for the respective standard deviation) in each of the selected biogeochemical provinces. Spring and autumn values are shown as dark and open circles, respectively. Significant regression lines (p <0.05) and regression slopes including the standard error are also given. Solid lines stand for spring results and dashed lines for autumn.

variability. Prior to making this analysis, all measurements were referenced to their respective months in the year 2005, which was arbitrarily chosen as the reference year. This adjustment consisted of adding or subtracting to each sample the xCO_2^{atm} difference between the date of the measurement and the one in 2005 as described in Sect. 2.3. The effect of temperature on the fCO_2^{sw} measurements was removed by normalising the observations to the mean in situ SST (Table 2) following Takahashi et al. (1993). This new normalised and corrected variable ($'fCO_2^{sw}$) was then used to estimate the biochemical control. The $'fCO_2^{sw}$ values were fitted with second-order multiple polynomials using SST and

chl *a* observations as described in Ono et al. (2004) and linear relationship with SSS and WS as independent variables according to the Eq. 4.

$$'fCO_2^{sw} = A + \sum_{i=1}^{2} \varphi_i (SST - \mu_{SST})^i + B(SSS - \mu_{SSS}) \quad (4)$$
$$+ CWS + \sum_{i=1}^{2} \beta_i (chla)^i$$

The multiple linear regression coefficients were obtained using a forward stepwise method where only parameters that accounted for at least 1% of the $'fCO_2^{sw}$ variability were included in the algorithm. The μ_{SST} and μ_{SSS} stand for averages value of SST and SSS for each province, respectively (Table 2). The regression coefficients for (4) and the percentage of normalized fCO_2^{sw} variability explained by each parameter in the different provinces are given in Table 3.

The empirical algorithm explained most of the $'fCO_2^{sw}$ variability of the separated provinces along the Atlantic Ocean. The fCO_2^{sw} changes observed in regions during spring and summer were correctly fitted and the root mean square errors ranged between 7.1 and 31.9 µatm estimated in the ENAS and SAC regions, respectively, in autumn (Table 3).

The main driver of the fCO_2^{sw} variability was SST in practically every region, with the exception of the surface waters of the equatorial provinces such as NEC in autumn and NECC during both seasons. SST was especially the main parameter explaining $'fCO_2^{sw}$ variability in the subtropical waters of both hemispheres reaching a maximum value of 85% in SAC region. The SST–$'fCO_2^{sw}$ correlations were mostly negative due to the lower pH values in warmer waters. Strong SST–$'fCO_2^{sw}$ relationships were observed in the provinces characterized by the upwelling and mixing of different waters (Table 3). As a result, the strongest relationships were found in the upwelling systems of the equator waters (SEC province in autumn; -34 ± 3 µatm °C^{-1}) and of the Southern Ocean (FC in March; -84 ± 3 µatm °C^{-1}).

In general terms, the effect of the observed SSS changes on $'fCO_2^{sw}$ was secondary. However the $'fCO_2^{sw}$ variability of tropical waters in autumn showed an important dependence of the SSS changes. The influence of SSS on fCO_2^{sw} reached a maximum value of 79% in the NECC region with a coefficient of 17.3 ± 0.3 µatm per SSS unit (Table 3). The SSS also accounted for 49% of the observed $'fCO_2^{sw}$ variability in spring in which the SSS minimum was located (Table 2). On the north, $'fCO_2^{sw}$ changes of the NEC region reproduced a similar seasonal influence of SSS explaining 11% and 62% in spring and autumn, respectively. The contribution of the SSS to the fCO_2^{sw} variability was also notable in the surface waters of the DP reaching an 10%.

Phytoplankton activity estimated via the chl *a* proxy showed a reduced influence on the $'fCO_2^{sw}$ variability that did not exceed 7%. This percentage was obtained in the ENAS region with a coefficient of -11.0 ± 0.5 µatm mg m^{-3} in autumn. Other regions sampled in the vicinity of the coastline such as STG and SAS region also showed a significant inverse $'fCO_2^{sw}$–chl *a* relationship that pointed out an important biological CO_2 uptake (Table 3). Remotely sensed chl *a* also had a notable influence on the fCO_2^{sw} of the FC region. However contrary to expectation, similar positive correlations between fCO_2^{sw}–chl *a* of 61 ± 11 and 67 ± 19 µatm mg m^{-3} were observed in March and November, respectively.

4 Discussion

The fourteen FICARAM cruises held between 2000 and 2008 have allowed us analyze the fCO_2^{sw} variability over seasonal and long-term scales and its biochemical forcing in spring and autumn. These underway measurements revealed a consistent pattern in the Northern Hemisphere but larger variability in the South Hemisphere (Figs. 2, 3) coinciding with the finding of Gruber et al. (2009) from analyzing anthropogenic fluxes. The consistency of these underway observations gathered on board of *R/V Hespérides* and *R/V Las Palmas* was studied comparing them with the recent climatology produced by Takahashi et al. (2009) (hereinafter; TC09). It is necessary to clarify that these cruises were not included in the construction of TC09 as other measurements calibrated with two standard gases (see Sect. 2.2). The co-location criteria of the monthly TC09 estimations meant that they did not differ temporally by more than 15 days and spatially by more than 355 km. The differences of ΔfCO_2 between those measured in the FICARAM cruises and TC09 ($\Delta\Delta fCO_2$') were corrected by taking into account the SST disagreements (ΔSST) and estimating $\Delta\Delta fCO_2$. The adjustment was carried out assuming theoretical temperature dependence in isochemical conditions such as described in Takahashi et al. (1993). Climatological k and S according to Eq. 3 multiplied $\Delta\Delta fCO_2$ in order to obtain FCO_2 differences between both datasets (ΔFCO_2). Table 4 shows the mean and standard deviation of these differences with the disagreements in SST (ΔSST) and SSS (ΔSSS).

In general terms, the FICARAM dataset showed warmer surface waters along the Atlantic Ocean with the exception of the Patagonian Sea than the reported by TC09 (Table 4). These disagreements were higher during the spring cruises reaching significant offsets. On the contrary, ΔSSS values were minimum with the exception of NECC and regions of the Patagonian Sea which are characterized by a large continental inputs and complex oceanography (Wanninkhof et al., 2007; Bianchi et al., 2009) and in which FICARAM cruises sampled less saline waters. ΔfCO_2 values along the Atlantic Ocean showed a statistically insignificant mean anomaly of -3 ± 18 µatm. This intensification in the CO_2 undersaturation yielded a small increase of 0.02 ± 0.14 mol m^{-2} yr^{-1} of the ocean uptake of atmospheric CO_2. In general terms, these

Table 3. Regression coefficients (in italics) and variability explained (bold-faced) by each of the parameters included in the empirical algorithm given in equation (4) applied in every biogeochemical province where $fCO_2^{sw}{}_0$ mean the start point. The root mean square (rms) and the correlation coefficient (r^2) are also given. The "n" value stands for the number of valid data included in each analysis.

Region	Season	rms µatm	$'fCO_2$ µatm n	sst-μ °C $r^{2\prime}$	(sst-μ)^2 $°C^2$	sss-μ	*ws* (m s^{-1})	chl *a* (mg m^{-3})	chl a^2 (mg m^3)^2
ENAS 39–27° N	spring	9.2	*361 ± 1* **2739**	*−15.2 ± 0.9* **60**		*25 ± 1* **3**	*−0.9 ± 0.1* **2**		*3.8 ± 0.4* **1**
	autumn	7.1	*372.9 ± 0.4* **5759**	*−6.8 ± 0.3* **68**	*−0.9 ± 0.1* **1**			*−11.0 ± 0.5* **7**	
CC 27–16° N	spring	11.8	*337 ± 2* ***1879***	−19 ± 1 **48**	−1.6 ± 0.2 **2**	6.5 ± 0.7 **2**	*3.1 ± 0.2* ***6***		9.1 ± 0.7 **2**
	autumn	13.3	*402.4 ± 1* **6091**	−16.9 ± 0.1 **74**	0.82 ± 0.07 **1**	5.7 ± 0.4	*−1.3 ± 0.1* **1**	−83 ± 3 **1**	47 ± 2 **1**
NEC 16–8° N	spring	10.4	*356 ± 2* ***685***	*−13.8 ± 8* ***79***		*41 ± 1* ***11***			
	autumn	13.2	*357 ± 1* **3734**	*−5.7 ± 0.3* **4**	*4.5 ± 0.6* **1**	*24.2 ± 0.4* **62**	*−0.9 ± 0.1* **1**	*73 ± 4* 1	*−72 ± 5* 3
NECC 8–1° N	spring	9.1	*308 ± 1* 903	*19 ± 1* ***15***	*4.6 ± 0.9* ***2***	*34 ± 1* ***49***	*4.5 ± 0.3* ***6***		*-21 ± 5* ***1***
	autumn	7.8	*345.2 ± 0.4* **3778**	*−16 ± 0.3* **7**		*17.3 ± 0.3* **79**	*2.0 ± 0.1* **3**	*48 ± 3* 1	
SEC 1° N–15° S	spring	10.7	*398 ± 4* 1586	*−34 ± 3* ***28***	*6 ± 1* ***1***	*−8.5 ± 0.6* ***7***	*2.3 ± 0.2* ***6***		
	autumn	12.8	*379 ± 1* **6169**	*−29.3 ± 0.5* **36**		*−23.7 ± 0.5* **16**			
STG 15–31° S	spring	12.2	*351 ± 8* **3164**		*−1.9 ± 0.1* **56**	*−18.3 ± 0.6* **11**			*83 ± 9* 1
	autumn	13.6	*389 ± 1* **4212**	*−12.5 ± 0.2* **58**		*7.1 ± 0.6* **1**	*−1.1 ± 0.1* **1**	*−49 ± 2* **4**	*14 ± 1* **2**
SAS 31–40° S	spring	13.4	*325.6 ± 0.5* **1584**	*−8.8 ± 1.1* **81**	*0.59 ± 0.03* **4**				
	autumn	19.5	*380 ± 4* **2434**	*−4.3 ± 0.5* **23**		*2.0 ± 0.4* **1**	*−2.8 ± 0.2* **7**	*−157 ± 32* **6**	
SAC 40–51° S	spring	17.5	355 ± 1 **1893**	−22.9 ± 0.2 **85**	1.00 ± 0.03 **4**	30 ± 1 **2**			87 ± 7 1
	autumn	31.9	*340 ± 8* **593**	*68 ± 4* **6**	*16.2 ± 0.8* **47**	*104 ± 8* **14**	*7.0 ± 0.6* **8**		
FC 51–56° S	spring	16.0	386 ± 6 **329**	−34 ± 3 **69**	−6 ± 2 **4**		−2.3 ± 0.3 **3**	61 ± 11 **4**	
	autumn	24.0	327 ± 5 **709**	−84 ± 3 **69**	−21 ± 2 **8**	21 ± 2 **5**	−3.5 ± 0.3 **5**	67 ± 19 **1**	
DP 56–66° S	autumn	12.4	339 ± 3 **1415**	−14.1 ± 0.2 **75**		86 ± 3 **10**		312 ± 42 1	

Table 4. Mean differences and standarad deviation ($\mu \pm \sigma$) of SST (ΔSST), SSS (ΔSSS), ΔfCO_2 ($\Delta\Delta fCO_2'$), FCO_2 (ΔFCO_2) between the monthly averaged estimations of the Takahashi's climatology (Takahashi et al., 2009) and these in situ measurements in the ocean waters during the FICARAM cruises ($X^{FICARAM} - X^{TC09}$). $\Delta\Delta fCO_2$ was estimated correcting $\Delta\Delta fCO_2'$ from ΔSST values and assuming the theoretical temperature control described by Takahashi et al. (1993). To compare the climatological FCO_2 values to our estimations, we multiplied $\Delta\Delta fCO_2$ with climatological k and S according to Eq. 3.

Region	Boreal Season	ΔSST °C	ΔSSS	$\Delta\Delta fCO_2'$ µatm	$\Delta\Delta fCO_2$ µatm	ΔFCO_2 mol m^{-2} yr^{-1}
ENAS	*spring*	0.2 ± 0.4	0.0 ± 0.2	-10 ± 6	-13 ± 7	-0.8 ± 0.5
39–27° N	autumn	*0.6 ± 0.4*	*0.1 ± 0.1*	*12 ± 7*	*3 ± 9*	0.2 ± 0.4
CC	*spring*	0.1 ± 0.3	0.0 ± 0.2	-5 ± 7	-7 ± 9	-0.4 ± 0.5
27–16° N	autumn	*0.6 ± 0.8*	*0.1 ± 0.2*	*10 ± 12*	*3 ± 11*	*0.1 ± 0.6*
NEC	*spring*	0.6 ± 0.4	-0.1 ± 0.1	-13 ± 12	-19 ± 11	-1.2 ± 0.7
16–8° N	autumn	*0.5 ± 0.5*	*−0.1 ± 0.3*	*−5 ± 12*	*−13 ± 12*	*−0.6 ± 0.6*
NECC	*spring*	0.5 ± 0.2	-0.3 ± 0.2	-9 ± 13	-16 ± 13	-0.8 ± 0.6
8°–1° N	autumn	*0.3 ± 0.5*	*−0.5 ± 0.4*	*−6 ± 12*	*−10 ± 17*	*−0.4 ± 0.5*
SEC	*spring*	0.2 ± 0.2	0.0 ± 0.2	2 ± 8	-6 ± 9	-0.3 ± 0.4
1° N–15° S	autumn	*0.1 ± 0.4*	*−0.1 ± 0.2*	*−2 ± 9*	*0 ± 13*	*0.0 ± 0.9*
STG	*spring*	1.0 ± 0.7	0.3 ± 0.3	6 ± 17	-10 ± 11	-0.4 ± 0.5
15–31° S	autumn	*0.5 ± 0.6*	*0.1 ± 0.2*	*2 ± 15*	*−4 ± 15*	*−0.3 ± 0.8*
SAS	*spring*	1.0 ± 0.6	0.0 ± 0.3	-1 ± 19	-16 ± 16	-1.1 ± 1.2
31–40° S	autumn	*−0.2 ± 0.6*	*0.4 ± 0.3*	*−15 ± 10*	*−12 ± 9*	*−1.0 ± 0.8*
SAC	*spring*	-1.8 ± 1.9	0.0 ± 0.1	-5 ± 16	23 ± 40	2.0 ± 3.4
40–51° S	autumn	*−0.9 ± 1.3*	*−0.2 ± 0.2*	*−20 ± 26*	*−13 ± 34*	*−1.1 ± 3.0*
FC	*spring*	-0.3 ± 0.5	-0.1 ± 0.1	8 ± 27	14 ± 32	1.7 ± 3.9
51–56° S	autumn	*−0.1 ± 0.6*	*−0.1 ± 0.3*	*−22 ± 35*	*−21 ± 43*	*−2.5 ± 5.3*
DP						
56–66° N	autumn	-0.9 ± 0.7	-0.1 ± 0.2	-27 ± 19	-13 ± 22	-1.5 ± 2.2

results support the consistency between both datasets and the validity of the CO_2 climatology along the Atlantic Ocean during spring and autumn seasons. However the comparison at regional scale showed some offsets that are detailed below.

The oceanic waters of the ENAS region in April showed significant intensification of 13 ± 7 µatm in the CO_2 undersaturation of the interpolated values from TC09 (Table 4). This difference under average conditions of solubility and transfer velocity reported by Takahashi et al. (2009) would produce an offset in the CO_2 uptake of 0.8 ± 0.5 mol m^{-2} yr^{-1}. Contrary to these disagreements in ΔfCO_2 and FCO_2 in spring, the near equilibrium status of these waters in autumn was closely reproduced by both databases showing a difference of 3 ± 9 µatm. $\Delta\Delta fCO_2$ values in the CC province also pointed out the agreement in the ΔfCO_2 observations (Table 4) in spite of the complex hydrography related to the intense upwelling events that characterize this region (Mittelstaedt, 1991). In this sense, long-term changes in the WS indicated a relaxation of the coastal upwelling (Roy and Reason, 2001) of -0.30 ± 0.07 m s^{-1} yr^{-1} in spring that it was even reproduced in a lesser extent in autumn. The direct WS–'fCO_2^{sw} relationship (Table 3) suggests an increase of the stratification and so, a reduction of the mixing processes with subsurface CO_2 rich waters. However any significant change directly related to upwelling processes was observed in other variables (Fig. 4b). As a result, the chl *a* signal was unlikely to have been detected in surface ocean waters because of its confinement to the coast at these latitudes (Arístegui et al., 2009) associated to limitation in the surface nitrate concentration (Lauthuilière et al., 2008). Nevertheless the chl *a* signal associated with the intense seasonal upwelling in the NEC province and to the south of Cape Blanc (10–19° N), extends to open ocean regions from February to May (Aristegui et al., 2009). The remotely retrieved observations

of chl *a* in this region showed a long-term spring decrease of $-0.03 \pm 0.01\,mg\,m^{-3}\,yr^{-1}$ as was reported by Gregg et al. (2005). This finding implies a net reduction of the biological CO_2 uptake (Table 3) during the spring cruises and also seems to explain the general year-to-year decrease of CO_2 saturation (Fig. 4b, c). Nevertheless and in spite of this ΔfCO_2 increase, spring ΔfCO_2 measurements that were mainly controlled by SST exceeded the climatological undersaturation close equilibrium status with the atmosphere (Takahashi et al., 2009). SSS changes controlled the ΔfCO_2 distribution in autumn in which $\Delta\Delta fCO_2$ reached an offset of 13 ± 12µatm leading the slight CO_2 outgassing of TC09 (Takahashi et al., 2009) to null role as sink or source (Table 2). Therefore the long-term changes of the subtropical waters of the North Atlantic Ocean in spite of not being statistically significant pointed out a reduction in outgassing (Fig. 4c) as was observed in the ESTOC site (Santana-Casiano et al., 2007).

In the light of these results, the analysis of the FICARAM dataset supports recent work reporting the weakening of the upwelling events in parallel to the decrease of primary production in the Canary upwelling system (Santos et al., 2005; Chavez and Messié, 2009; Pérez et al., 2010). The relaxation of the Atlantic trade winds is directly linked to the decrease of the pressure gradient between the Azores High and the Icelandic Low. This scenario is described by the negative index of the NAO (Hurrell et al., 1995) that prevailed during the sampling period of FICARAM cruises. Apart from explaining the observed WS declination in this region of the North Atlantic, this large-scale climatic phenomenon is also related to the northward displacement of the waters from Azores current into the temperate regions (Flatau et al., 2003; Siedler et al., 2005; Häkkinen and Rhines, 2009). The northward advection of these waters is linked to several changes of the different biogeochemical variables in the North Atlantic Ocean (Marshall et al., 2001). Amongst others, warming of surface waters in the eastern tropical and subtropical gyre was associated with the NAO declination (Marshall et al., 2001; Santana-Casiano et al., 2007). Under this scenario, ΔfCO_2 would also increase reducing the ocean uptake of atmospheric CO_2 (Patra et al., 2005; Schuster et al., 2009), such as it was observed in the North Atlantic waters (Schuster and Watson, 2007; Thomas et al., 2008; Herbaut and Houssais, 2009). The analysis of the FICARAM cruises mostly reproduced these changes over decadal scale showing a faster increase of the fCO_2^{sw} in relation to the trend of atmospheric CO_2. Even the time delay beyond its maximum period of influence from December to March (Osborn, 2007), that is, during the spring cruises, linked to impact on physical and biological processes (Patra et al., 2005) affected autumn FCO_2 as well. However the long-term analysis did not show a SSS declination related to the northward advection of less saline waters (Santana-Casiano et al., 2007). Notwithstanding the direct influence of the NAO index on the water mass distribution affecting fCO_2^{sw} in the region (Lauvset et al., 2010), the presence of upwelled waters makes it difficult to interpret these results (Fig. 2a, b). The $\Delta\Delta fCO_2$ estimations in these regions should predominantly be positives as result of the comparison between ΔfCO_2 of a prevailing negative NAO period and average ΔfCO_2 values from different NAO scenarios gathered in TC09. Nevertheless the reduced number of the FICARAM cruises in these complex regions did not appropriately reproduce the monthly averages of the coarse grid of TC09 (Takahashi et al., 2009). Disagreements were especially notable in spring in which ΔfCO_2 reaches a short minimum as result of the single spring bloom (Santana-Casiano et al., 2007).

The tropical waters of the eastward flowing NECC region also showed lower ΔfCO_2 values and consequently, a reduction of the CO_2 outgassing, during the FICARAM cruises in both seasons. In spite of these differences, significant offset of -16 ± 13 µatm was only found in spring and reduced the role of these waters as CO_2 source in TC09 by $0.8 \pm 0.6\,mol\,m^{-2}\,yr^{-1}$. The supersaturation in autumn was also underestimated, namely, by -10 ± 17 µatm, yielding a difference of $-0.4 \pm 0.5\,mol\,m^{-2}\,yr^{-1}$. Both ΔfCO_2 disagreements coincided with important SSS differences of 0.5 ± 0.4 and 0.3 ± 0.2 in spring and autumn, respectively. The effect of ΔSSS on the CO_2 solubility and carbonic acid dissociation constants (Takahashi et al., 1993) was not considered in the estimation of $\Delta\Delta fCO_2$ as it was done for ΔSST. Nevertheless, this correction would be inversely proportional to the ΔSSS and it would only increase the observed disagreement by around 1 µatm. However the estimation of empirical relationships that correctly fitted in fCO_2^{sw} distribution in both seasons (Table 3) has identified the role of the SSS changes as an important driver of ΔfCO_2 variability. The impact of the SSS changes on the ΔfCO_2 distribution was especially outstanding in autumn, when they explained 79% of the variability of the estimated 'fCO_2^{sw} values with a coefficient of 17.3 ± 0.3 µatm per SSS unit (Table 3). Therefore less saline waters attributed to the discharges of the Orinoco, Parana and Amazon rivers (Müller-Karger et al., 1988; Ternon et al., 2000; Wanninkhof et al., 2007) and the intensification of eastward currents (Richardson and McKee, 1984) seemed to strongly lead the ΔfCO_2 changes, especially in autumn. Continental inputs fertilizing the surface tropical waters and stimulating the biological CO_2 drawdown would explain the positive estimated 'fCO_2^{sw} – SSS relationships, that is, the observed direct control on ΔfCO_2 (Lefèvre et al., 1998; Subramanian et al., 2008). Reinforcing this supposition, SSS decreases during the autumn cruises (Fig. 4) were observed in parallel to a significant reduction of CO_2 saturation and outgassing in $-3.5\,\mu atm\,yr^{-1}$ and $-0.09 \pm 0.03\,mol\,m^{-2}\,yr^{-2}$, respectively. The interannual fluctuations of the discharges of Orinoco, Parana and Amazon Rivers showed different relationships with large-scale alterations of the atmospheric pressure. In any case, Orinoco shows some relationship with these climatologic indicators (Hastenrath, 1990) while Parana discharges that

showed stationary positive correlations with NAO are intermittently influenced by ENSO (Labat et al., 2005). On the other hand, the discharges of the Amazon River show an important and nearly permanent inverse correlation with the ENSO (Zeng, 1999; Labat et al., 2005). In spite of the key control that plays these climatic indexes, the long-term SSS decrease and its influence on the ΔfCO_2 changes in NECC are difficult to interpret from NAO and ENSO considering the prevailing negative NAO period and a predominant positive ENSO scenario that dominated the FICARAM period.

The SEC region that closely interacts with the NECC region through the meridional displacements of the InterTropical Convergence Zone was characterized by higher ΔfCO_2 (Table 2) than the tropical waters further north (Goyet et al., 1998; Takahashi et al., 2009). The strong CO_2 supersaturation of this region was markedly similar to both FICARAM and TC09 datasets (Table 3). ΔfCO_2 and FCO_2 in autumn showed slight underestimations of -6 ± 9 µatm and -0.3 ± 0.4 mol m^{-2} yr^{-1}, respectively, while $\Delta\Delta fCO_2$ in spring was negligible (0 ± 13 µatm) representing ΔfCO_2 values of 0.0 ± 0.9 mol m^{-2} yr^{-1}. The spring agreements in the equatorial upwelling system that were the highest observed along the Atlantic Ocean were observed in parallel to significant changes at long-term scale. So, trade equatorial winds in the western basin of the South Atlantic showed a relaxation in parallel to the warming of the surface waters (Fig. 4e). The WS and SST anomalies in the tropical Atlantic over interannual scales were significantly related to the ENSO phenomenon (Enfield and Mayer, 1997; Latif and Grötzner, 2000). Consequently, positive SST anomalies prevail over the western equatorial Atlantic during the warm ENSO events as result of a reduction in the speed of trade winds. These long-term drifts seem to be connected to the response of the decreasing upwelling intensity that directly affects to the thermocline depth (Grodsky et al., 2008). Furthermore the teleconnection between Pacific and Atlantic Oceans is clearly evident during the boreal spring (Enfield and Mayer, 1997) as evident in the FICARAM cruises as well.

The seasonal CO_2 outgassing and absorption of the STG region in spring and autumn (Takahashi et al., 2009), respectively, were correctly reproduced by the FICARAM cruises (Table 3). Nevertheless poor agreements were observed during spring in spite of most values of Table 4 showing consistent results. So, FICARAM dataset roughly pointed out 23 °C (Fig. 2, 3; Table 2) determined by Ito et al. (2005) as the boundary between if the oceanic waters of the STG region acted as sink or source of CO_2 for the atmosphere. The SST changes yielded a considerable effect on fCO_2^{sw} (Ito et al., 2005) with a relative importance of SSS and chl *a* in spring and autumn, respectively (Table 3).

Nevertheless SAS region that acted as a strong sink of atmospheric CO_2 (Bianchi et al., 2009) showed significant offsets in October with values of $\Delta\Delta fCO_2$ and ΔfCO_2 of -12 ± 9 µatm and -1.0 ± 0.8 mol m^{-2} yr^{-1}, respectively (Table 4). Strong SSS anomalies of 0.4 ± 0.3 were found at the same month, which coincides with the most intense discharges of River Plate (Guerrero et al., 1997). Similar increases of -1.1 ± 1.2 mol m^{-2} yr^{-1} were observed during boreal spring with no average SSS differences. Results of the empirical estimation of the biochemical forcing showed a minimum influence of SSS on the ΔfCO_2 variability in both seasons. The ΔfCO_2 distribution was mostly controlled by the SST variability, especially in March, when it explained 85% of 'fCO_2^{sw} variability (Table 3). The fCO_2^{sw} distribution in November was controlled by SST with WS and chl *a* variables even though only 37% of fCO_2^{sw} changes were explained by these variables. So, the notable weight of the Plata River in the SAC region in autumn (Gordon, 1989) affecting the nutrient inputs (Bakun and Parrish, 1991) and controlling the production of chl *a* in the Patagoninan Sea (Froneman et al., 1999) was not properly accounted for using this simplistic approach.

The southern surface waters of the Patagonian Sea were systematically colder than the reported by TC09 reaching the lowest ΔSST of -1.8 ± 1.9 °C in SAC region during March cruises. The $\Delta\Delta fCO_2$ and ΔfCO_2 values of these waters in March showed notable supersaturation of 23 ± 40 µatm of FICARAM dataset that underestimated the climatological CO_2 uptake (Takahashi et al., 2009) in 2.0 ± 3.4 mol m^{-2} yr^{-1} (Table 4). Conversely the undersaturation of these waters was overestimated by -13 ± 34 µatm in October. The differences between in situ fCO_2^{sw} and values from empirical relationships were also maximum in the Patagonian Sea, with differences of 31.9 µatm being found in SAC waters during the autumn cruises (Table 3). Apart from the low number of measurements used to characterize these regions in both dataset, these disagreements reflect the complex hydrography and the heterogeneous fCO_2^{sw} distribution (Bianchi et al., 2005). Nevertheless some typical features of these waters were correctly described such as the notable outflow of the continental ice melting in the Pacific coast of Tierra de Fuego through the Magellan Strait (Fig. 2b, c; Piola and Rivas, 1997). These freshwater inputs enrich the surface nutrient concentration supporting the spring phytoplankton bloom and resulting in the observed CO_2 undersaturation of the coastal and ocean waters (Table 2; Romero et al., 2006). Nevertheless 'fCO_2–chl *a* relationships of the FC region far from representing phytoplankton CO_2 consumption showed similar positive values that were attributed to CO_2 inputs from continental inputs or remineralization processes. The non-synoptic sampling strategies followed in the FICARAM project could cause positive coefficients during the monitoring of senescent phytoplankton community. In relation to the long-term trends observed in these waters, the atmospheric pressure changes of the Southern Ocean represented by SAM could explain some of the observed interannual drifts. SAM variability that is related the Southern Ocean circulation through meridional shifts in the wind patterns (Hartamann and Lo; 1998) significantly affects biogeochemical

cycling and FCO_2 (Lovendrusky et al., 2007) of the Patagonian Sea. Therefore the significant WS weakness reported at these latitudes (Fig. 4g, h) could directly be associated with positive SAM values, which showed a slight increase during the FICARAM period. Warm SST anomalies and an increase of CO_2 outgassing that are also driven by positive phases of the SAM (Lovendrusky et al., 2007) could approximately be noticed from year 2005 as well (Fig. 4 g, h and i).

The DP region was crossed during two FICARAM cruises that only gathered underway measurements in November. The average ΔfCO_2 of -20 ± 11 µatm measured in the ocean waters (Table 2) described this branch of the Southern Ocean as a sink of atmospheric CO_2 (Metzl et al., 1999). This value is 13 ± 22 µatm lower than the climatological ΔfCO_2 (Takahashi et al., 2009) which showed an average outgassing of 10 µatm for this month. The FICARAM observations that came to findings of the different approaches (Metzl et al., 1999; Metzl, 2004; Gurney et al., 2002; Roy et al., 2003; McNeil et al., 2007) confirmed in the role of these waters as a sink of atmospheric CO_2 that was reported by Gruber et al. (2009). The CO_2 undersaturation of these waters showed a notable interannual variability as was found by Metzl (2004). The found ΔfCO_2 shift (Fig. 3b) between both Novembers can be explained by changes in thermohaline properties (Fig. 2b, d). So, colder and saltier waters in 2007 pointed to an intensification of the upwelling of North Atlantic Deep Water (Nowlin and Klink and, 1986) that led ΔfCO_2 values close to equilibrium status (Fig. 3b). On the other hand, warmer and less saline waters in 2008 showed a southward growing undersaturation that caused a CO_2 uptake of -1.8 ± 1.2 mol m^{-2} yr^{-1}. This intense CO_2 absorption, which was associated with photosynthetic activity of 0.17 ± 0.01 mg m-3, was also linked to the entrance of deep waters that increased the surface iron concentration (Metzl et al., 1991; Legendre et al., 1992; Poisson et al., 1994; Arrigo et al., 1997). This is somewhat lower phytoplanktonic community activity than reported during the spring bloom in the subAntarctic coastal area (Perissinotto et al., 2000; Blain et al., 2001; Delille et al., 2007). South of the Continental Water Boundary ($\sim$62° S; Fig. 2d) and where lowest ΔfCO_2 values were found, the role of surface waters change from a source to a sink of atmospheric CO_2. Consequently ΔfCO_2 of shelf waters of the Livingston Island showed a coastward increase in parallel to SSS that reached 27 µatm causing an outgassing of 0.8 mol m^{-2} yr^{-1} (Fig. 3b, d).

5 Summary

The FICARAM programme has proved to be a new source of information about the changing air-se CO_2 fluxes in the Atlantic Ocean. Moveover FICARAM cruises represented a unique opportunity to analyze from a quasi-synoptic point of view underway fCO_2^{sw} measurements in spring and autumn along an ample array of hydrographic regions of both Hemispheres. These measurements of the FICARAM cruises, that were independent of the surface ocean CO_2 atlas recently constructed by Takahashi et al. (2009), mostly reproduced the climatological estimations showing a mean ΔfCO_2 difference of -3 ± 18 µatm. This reduction in the CO_2 saturation of the surface waters represented an increase of 0.02 ± 0.14 mol m^{-2} yr^{-1} in the ocean uptake of atmospheric CO_2. Moreover fCO_2^{sw} measurements have allowed the detection of some changes in the long-term trends of the fluxes in some regions of the Atlantic Ocean. Shelf regions were also sampled along the coasts of Africa and South America. In general terms, the shelf waters repeated the behave of the adjacent waters even though emphasizing the observed results in both spring and autumn. The most remarkable results obtained are:

1. The Northern Subtropical Gyre acted as a sink of atmospheric CO_2 during the successive spring seasons (-1.8 ± 1.2 mol m^{-2} yr^{-1}) and as a source during autumn (0.2 ± 0.4 mol m^{-2} yr^{-1}). Similarly, the subtropical waters of the Southern Hemisphere absorbed CO_2 under spring conditions (-0.2 ± 0.7 mol m^{-2} yr^{-1}), while CO_2 outgasing occurred during autumn (0.6 ± 0.6 mol m^{-2} yr^{-1}). The seasonal distribution of fCO_2^{sw} in these latitudes was mainly determined by changes in SST that explained more than 80% of the fCO_2^{sw} variability, according to the proposed algorithm. Negative NAO scenario that prevailed during the sampling period of FICARAM cruises was linked to long-term declination of WS (0.30 ± 0.07 m s^{-1} y^{-1}) and chl *a* (0.03 ± 0.01 mg m^{-3} y^{-1}) that reinforce works reporting the weakening of the upwelling events in the Canary upwelling system (Santos et al., 2005; Chavez and Messié, 2009; Pérez et al., 2010). Under this pressure pattern of the North Atlantic Ocean, FICARAM measurements roughly pointed out the expected warming and the reduction of the ocean uptake of atmospheric CO_2.

2. Tropical waters were virtually in equilibrium with the atmosphere during spring and autumn, which yielded trifling air-sea CO_2 fluxes, especially in the NECC region. The analysed property distributions in the latter province revealed a significant long-term decrease of SSS (-0.16 ± 0.01 yr^{-1}) during the successive autumn cruises. At the same time, outstanding ΔfCO_2 reduction (-3.5 ± 0.9 µatm yr^{-1}) and a rise of oceanic CO_2 uptake (-0.09 ± 0.03 mol m^{-2} yr^{-1}). These strong SSS changes produced by the Amazon River outflows accounted for 79% of the observed fCO_2^{sw} variability in autumn and 49% in spring, providing uplift to the role of freshwater discharges in the uptake of CO_2.

3. To the south of the equator, the tropical waters of the equatorial upwelling system were highly supersaturated, exceeding the atmospheric CO_2 concentration

in spring and autumn by 24 ± 12 and 30 ± 11 µatm, respectively. These CO_2supersaturations represented a spring – autumn range of CO_2 outgassing that eventually reached southern latitudes in autumn of 0.7 ± 0.5 and $1.0 \pm 0.7\,\mathrm{mol\,m^{-2}\,yr^{-1}}$ in spring. An interannual surface warming of $0.11 \pm 0.03\,^{\circ}\mathrm{C\,yr^{-1}}$ and a WS decrease of $-0.58 \pm 0.14\,\mathrm{m\,s^{-1}\,yr^{-1}}$ characterized these waters during the successive spring cruises, which suggest the weakening of upwelling (Grodsky et al., 2008) that was directely associated with the warm ENSO events that dominated the FICARAM period (Enfield and Mayer, 1997; Latif and Grötzner, 2000).

4. The majority of provinces in the Patagonian Sea were systematically colder than the reported by Takahashi et al. (2009) and behaved as an intense sink of CO_2 in both southward or northward cruises. In particular, oceanic waters of the SAC province were the strongest CO_2 sink registered by the FICARAM cruises, namely, $-5.4 \pm 3.6\,\mathrm{mol\,m^{-2}\,yr^{-1}}$ in November. The heterogeneous distributions of ΔfCO_2 and FCO_2 in the Patagonian shelf were not well explained by either SST, SSS or chl a. The complex hydrography (Bianchi et al., 2005) and the scarce cruises held in this region yielded the worst adjustment of the fCO_2^{sw} observations.

5. The ocean branch of the Antarctic waters sampled in the Drake Passage in November were CO_2 undersaturated in -20 ± 11 µatm. These oceanic waters displayed an average uptake rate of $-1.1 \pm 0.9\,\mathrm{mol\,m^{-2}\,yr^{-1}}$ that were characterized by a notable change between the November of 2007 and the November 2008. On the other hand, the distal shelf of the Livingston Island acted as a slight source of CO_2 to the atmosphere ($0.1 \pm 0.3\,\mathrm{mol\,m^{-2}\,yr^{-1}}$).

Acknowledgements. We would like to extend our gratitude to the Captains and crew of B/O Hespérides and B/O Las Palmas for their hospitality and essential help, and to the UTM team for their logistic support. We are especially grateful to Iago Rodicio and Marcos Villafn who occupied of the IT support throughout the nine years of FICARAM cruises. We also thank to Adrian Callaghan and Jonathan Bares for substantially improving the writing style of the manuscript. Three anonymous reviewers provided valuable comments and suggestions to a first version of the manuscript. This study was developed and funded by the European Commission within the 6th Framework Programme (EU FP6 CARBOOCEAN Integrated Project, Contract no. 511176), the Spanish research project FICARAM (CICYT. REN 2000-2467-E and 2001-4839-E), Ministerio de Ciencia e Innovación (CTM2006–27116–E/MAR) and Xunta de Galicia (PGIDIT05PXIC40203PM).

Edited by: A. V. Borges

References

Andersson, A. J. and Mackenzie, F. T.: Shallow-water oceans: a source or sink of atmospheric CO_2? Frontiers in Ecology and Environment, 2(7), 348–353, 2004.

Arístegui, J., Barton, E. D., Álvarez-Salgado, X. A., Santos, A. M. P., Figueiras, F. G., Kifani, S., Hernández-León, S., Mason, E., Machú, E., and Demarcq, H.: Sub-regional ecosystem variability in the Canary Current upwelling, Prog. Oceanogr., 83, 33–48, 2009.

Bakun, A. and Parrish, R. H.: Comparative studies of coastal pelagic fish reproductive habitats: the anchovy (Engraulis anchoita) of the southwestern Atlantic, ICES Journal of Marine Science: J. Conseil, 48, 343-361, 1991.

Bakun, A., Field, D. B., Redondo-Rodriguez, A., and Weeks, S. J.: Greenhouse gas, upwelling-favorable winds, and the future of coastal ocean upwelling ecosystems, Glob. Change Biol., 16, 1213–1228, doi:10.1111/j.1365-2486.2009.02094.x, 2010.

Barton, E. D.: Ocean Currents: Atlantic Eastern Boundary – Canary Current/ Portugal Current, in: Encyclopedia of Ocean Sciences, edited by: Steele, J., Thorpe S., and Turekian, K., Vol. 1, pp 380–389, Academic Press, London, 2001.

Battle, M., Bender, M. L., Tans, P. P., White, J. W. C., Ellis, J. T., Conway, T., and Francey, R. J.: Global carbon sinks and their variability inferred from atmospheric O_2 and δC^{13}, Science, 287, 2467–2470, 2000.

Bianchi, A. A., Giulivi, C. F., and Piola, A. R.: Mixing in the Brazil-Malvinas confluence, Deep-Sea Res. Pt. II, 40, 1345–1358, 1993.

Bianchi, A. A., Bianucci, L., Piola, A. R., Pino, D. R., Schloss, I., Poisson, A., and Balestrini, C. F.: Vertical stratification and air-sea CO_2 fluxes in the Patagonian shelf, J. Geophys. Res.-Oceans, 110, C07003, doi:10.1029/2004JC002488, 2005.

Bianchi, A. A., Pino, D. R., Perlender, H. G. I., Osiroff, A. P., Segura, V., Lutz, V., Clara, M. L., Balestrini, C. F., and Piola, A. R.: Annual balance and seasonal variability of sea-air CO_2 fluxes in the Patagonia Sea: Their relationship with fronts and chlorophyll distribution, J. Geophys. Res.-Oceans, 114, C03018, doi:10.1029/2008JC004854, 2009.

Blain, S., Tréguer, P., Belviso, S., Bucciarelli, E., Denis, M., Desabre, S., Fiala, M., Martin Jézéquel, V., Le Fèvre, J., and Mayzaud, P.: A biogeochemical study of the island mass effect in the context of the iron hypothesis: Kerguelen Islands, Southern Ocean, Deep-Sea Res. Pt. I, 48, 163–187, 2001.

Borges, A. V., Tilbrook, B., Metzl, N., Lenton, A., and Delille, B.: Inter-annual variability of the carbon dioxide oceanic sink south of Tasmania, Biogeosciences, 5, 141–155, 2008, http://www.biogeosciences.net/5/141/2008/.

Canadell, J. G., Le Quéré, C., Raupach, M. R., Field, C. B., Buitenhuis, E. T., Ciais, P., Conway, T. J., Gillett, N. P., Houghton, R. A., and Marland, G.: Contributions to accelerating atmospheric CO_2 growth from economic activity, carbon intensity, and efficiency of natural sinks, P. Natl. A. Sci., 104, 10288–10293, 2007.

Chavez, F. P. and Messié, M.: A comparison of Eastern Boundary Upwelling Ecosystems, Prog. Oceanogr., 83, 80–96, 2009

Chen, C. T. A. and Borges, A. V.: Reconciling opposing views on carbon cycling in the coastal ocean: Continental shelves as sinks and near-shore ecosystems as sources of atmospheric CO_2, Deep-Sea Res. Pt. II, 56, 578–590, doi:10.1016/j.dsr2.2009.01.001, 2009.

Cooper, D. J., Watson, A. J., Ling, R. D.: Variations of pCO_2 along

a North Atlantic shipping route (UK to Jamaica): a year of automated observations, Mar. Chem., 60, 147–164, 2008.

Delille, D., Gleizon, F., and Delille, B.: Spatial and temporal variation of bacterioplankton in a sub-Antarctic coastal area (Kerguelen Archipelago). J. Marine Syst., 68, 366–380, 2007.

Emery, W. J. and Dewar, J. S.: Mean temperature-salinity, salinity-depth and temperature-depth curves for the North Atlantic and the North Pacific, Prog. Oceanogr., 11, 219–305, 1982.

Enfield, D. and Mayer, D.: Tropical Atlantic sea surface temperature variability and its relation to El Niño-Southern Oscillation, J. Geophys. Res., 102(C1), 929–945, 1997.

Flatau, M. K., Talley, L., and Niiler, P. P.: The North Atlantic Oscillation, surface current velocities, and SST changes in the subpolar North Atlantic, J. Climatol., 16, 2355–2369, 2003.

Francey, R. J., Tans, P. P., Allison, C. E., Enting, I. G., White, J. W. C., and Trolier, M.: Changes in oceanic and terrestrial carbon uptake since 1982, Nature, 373, 326–330, 1995.

Froneman, P. W., McQuaid, C. D., and Laubscher, R. K.: Size-fractionated primary production sudies in the vicinity of the Subtropical Front and an adjacent warm-core south of Africa in austral winter, J. Plankton Res., 21, 2019-2035, 1999.

Gordon, A. L.: Brazil-Malvinas confluence-1984, Deep-Sea Res. Pt. II, 36, 359–384, 1989.

Goyet, C., Adams, R., and Eischeid, G.: Observations of the CO_2system properties in the tropical Atlantic Ocean. Mar. Chem., 60, 49–61, 1998.

Gregg, W. W, Casey, N. W., and McClain, C. R.: Recent trends in global ocean chlorophyll, Geophys. Res. Lett., 32, L03606, doi:10.1029/2004GL021808, 2005.

Grodsky, S. A., Carton, J. A., McClain, C. R.: Variability of upwelling and chlorophyll in the equatorial Atlantic, Geophys. Res. Lett., 35, L03610, doi:10.1029/2007GL032466, 2008.

Gruber, N., Gloor, M., Mikaloff Fletcher, S. E., Doney, S. C., Dutkiewicz, S., Follows, M. J., Gerber, M., Jacobson, A. R., Joos, F., Lindsay, K., Menemenlis, D., Mouchet, A., Müller, S. A., Sarmiento, J. L., and Takahashi, T.: Oceanic sources, sinks, and transport of atmospheric CO_2, Global Biogeochem. Cy., 23, GB1005, doi:10.1029/2008GB003349, 2009.

Guerrero, R., Acha, E., Framinan, M., and Lasta, C.: Physical oceanography of the River Plate Estuary, Cont. Shelf Res., 17, 727–742, 1997.

Gurney, K. R., Law, R. M., Denning, A. S., Rayner, P. J., Pak, B. and the TransCom-3L2 modelers.: Transcom-3 inversion intercomparison: Control results for the estimation of seasonal carbon sources and sinks, Global Biogeochem. Cy., 18, GB1010, doi:10.1029/2003GB002111, 2004.

Hartmann, D. L. and Lo, F.: Wave-Driven Zonal Flow Vacillation in the Southern Hemisphere, J. Atmos. Sci., 55(8), 1303–1315, 1998.

Häkkinen, S. and Rhines, P. B.: Shifting surface currents in the northern North Atlantic Ocean, J. Geophys. Res.-Oceans, 114 (C04005), doi:10.1029/2008JC004883, 2009.

Herbaut, C. and Houssais, M. N.: Response of the eastern North Atlantic subpolar gyre to the North Atlantic Oscillation, Geophys. Res. Lett., 36, L17607, doi:10.1029/2009GL039090, 2009.

Hill, A. D., Hickey, B. M., Shillington, F. A., Strub, P. T., Brink, K. H., Barton, E., and Thomas, A. C.: Eastern ocean boundaries, Coastal segment (E), The Sea, 11, 29–65, 1998.

Hooker, S. B., Rees, N. W., and Aiken, J.: An objective methodology for identifying oceanic provinces, Prog. Oceanogr., 45, 313–338, 2000.

Hooker, S. B., Esaias, W. E., Feldman, G. C., Gregg, W. W., and McClain, C. R.: An overview of SeaWiFS and ocean colour, edited by: Hooker, S. B. and Firestone, E. R., NASA Technical Memo 104566, vol. 1. NASA Goddard Space Flight Centre, Greenbelt, MA, p. 24, 1992.

Houghton, R. A.: Revised estimates of the annual net flux of carbon to the atmosphere from changes in land use and land management 1850–2000, Tellus B, 55, 378–390, doi:10.1034/j.1600-0889.2003.01450.x, 2003.

Hurrell, J. M.: Decadal trends in the North Atlantic oscillation regional temperatures and precipitation, Science, 269, 676–679, 1995.

Ito, R. G., Schneider, T. B., and Thomas, H.: Distribution of surface fCO2 and air–sea fluxes in the Southwestern subtropical Atlantic and adjacent continental shelf, J. Marine Syst. 56, 227–242, 2005.

Kalnay, E., Kanamitsu, M., Kistler, R., Collins, W., Deaven, D., Gandin, L., Iredell, M., Saha, S., White, G., and Woollen, J.: The NCEP/NCAR reanalysis project, B. Am. Meteorol. Soc., 77, 437–471, 1996.

Keeling, C. D.: Carbon dioxide in surface ocean waters, Global distribution, J. Geophys. Res., 73, 4543–4553, 1968.

Keeling, C. D., Whorf, T. P., Wahlen, M., and Plicht, J.: Interannual extremes in the rate of rise of atmospheric carbon dioxide since 1980, Nature, 375, 666–670, 1995.

Keeling, C. D. and Whorf, T. P.: The 1800-year oceanic tidal cycle: A possible cause of rapid climate change: Natl. A. Sci. P., 97(10), 3814–3819, 2000.

Körtzinger, A., Thomas, H., Schneider, B., Gronau, N., Mintrop, L., and Duinker, J. C.: At-sea intercomparison of two newly designed underway pCO_2 systems – encouraging results, Mar. Chem., 52, 133–145, 1996.

Labat, D., Ronchail, J., and Guyot, J. L.: Recent advances in wavelet analyses: Part 2 – Amazon, Parana, Orinoco and Congo discharges time scale variability, J. Hydrol., 314(1–4), 289–311, 2005.

Latif, M. and Grötzner, A.: The equatorial Atlantic oscillation and its response to ENSO, Clim. Dynam., 16, 213–218, 2000.

Lauvset, S. K., Olsen,A., Wanninkhof, R., Takahashi, T., Borges, A. V., Cai, W. -J., Skjelvan, I., Padin, X. A., Perez, F. F., Rios, A. F., Lefevre, N., Dandonneau, Y., Gonzalez-Davila, M., Johannessen, T., Körtzinger, A., Pierrot, D., Santana-Casiano, J. M., Schuster, U., Steinhoff, T., Wallace, D. and Watson, A.: North Atlantic relationships between surface fCO_2 and hydrography, evaluated using fCO_2-SST relationships, Deep Sea Res., in press, 2010.

Lauthuilière, C., Echevin, V., and Lévy, M.: Seasonal and intraseasonal surface chlorophyll-a variability along the northwest African coast, J. Geophys. Res., 113, C05007. doi:10.1029/2007JC004433, 2008.

Lefèvre, N.: Objective mapping of the seasonal variability of ΔpCO_2 in the North Atlantic Ocean, The Global Atmosphere and Ocean System, 5, 247–271, 1997.

Lefèvre, N., Moore, G., Aiken, J., Watson, A., Cooper, D., and Ling, R.: Variability of pCO_2 in the tropical Atlantic in 1995, J. Geophys. Res., 103, 5623–5634, 1998.

Lefèvre, N., Watson, A. J., Olsen, A., Ríos, A. F., Pérez, F. F.,

and Johannessen, T.: A decrease in the sink for atmospheric CO_2 in the North Atlantic, Geophys. Res. Lett., 31, L07306, doi:10.1029/2003GL018957, 2004.

Legendre, L., Ackley, S. F., Dieckmann, G. S., Gulliksen, B., Horner, R., Hoshiai, T., Melnikov, I. A., Reeburgh, W. S., Spindler, M., and Sullivan, C. W.: Ecology of sea ice biota, Polar Biol., 12, 429–444, 1992.

Longhurst, A., Sathyendranath, S., Platt, T., and Caverhill, C.: An estimate of global primary production in the ocean from satellite radiometer data, J. Plankton Res., 17, 1245–1271, 1995.

Lovenduski, N. S., Gruber, N., Doney, S. C., and Lima, I. D.: Enhanced CO_2 outgassing in the Southern Ocean from a positive phase of the Southern Annular Mode, Global Biogeochem. Cy., 21(2), GB2026, doi:10.1029/2006GB002900, 2007.

Lueger, H., Wanninkhof, R., Olsen, A., Triñanes, J., Johannessen, T., Wallace, D. W. R., and Körtzinger, A.: The Sea-Air CO_2 Flux in the North Atlantic Estimated From Satellite and ARGO Profiling Float Data, NOAA Tech. Memo. OAR AOML-96, 28 pp., Atlantic Oceanography and Meteorological Laboratory, NOAA, Miami, Fla, 2008.

Marshall, J., Kushnir, Y., Battisti, D., Chang, P., Czaja, A., Dickson, R., Hurrell, J., McCartney, M., Saravanan, R., Visbeck, M.: North Atlantic climate variability, phenomena, impacts and mechanisms, International J. Climatol., 21, 1863–1898, 2001.

McNeil, B. I., Metzl, N., Key, R. M., Matear, R. J., and Corbiere, A.: An empirical estimate of the Southern Ocean air-sea CO_2 flux, Global Biogeochem. Cy., 21, GB3011, doi:10.1029/2007GB002991, 2007.

Metzl, N., Beauverger, C., Brunet, C., Goyet, C., and Poisson, A.: Surface water carbon dioxide in the southwest Indian sector of the Southern Ocean: a highly variable CO_2 source/sink region in summer, Mar. Chem., 35, 85–95, 1991.

Metzl, N., Tilbrook, B., and Poisson, A.: The annual fCO_2 cycle and the air-sea CO_2 flux in the sub-Antarctic Ocean, Tellus B, 51, 849–861, 1999.

Metzl, N.: Air-sea CO_2 fluxes in the Southern Ocean: natural and methodological variabilities, SOLAS Open Conference, Halifax, 2004.

Mittelstaedt, E.: The ocean boundary along the northwest African coast: circulation and oceanographic properties at the sea surface, Prog. Oceanogr., 26, 307–355, 1991.

Müller-Karger, F. E., McClain, C. R., and Richardson, P. L.: The dispersal of the Amazon's water, Nature, 333, 56–59, 1988.

Nowlin, W. D. and Klinck, J. M.: The physics of the Antarctic Circumpolar Current, Geophys. Res. Lett., 24, 469–491, 1986.

Olsen, A., Trinanes, J. A., and Wanninkhof, R.: Sea–air flux of CO_2 in the Caribbean Sea estimated using in situ and remote sensing data, Remote Sens. Environ., 89, 309–325, 2004.

Ono, T., Saino, T., Kurita, N., and Sasaki, K.: Basin-scale extrapolation of shipboard pCO_2 data by using satellite SST and Chla, Int. J. Remote Sens., 25(19), 3803–3815, 2004.

Osborn, T.: North Atlantic Oscillation index data, http://www.cru.uea.ac.uk/~timo/projpages/nao_update.htm, 2010.

Padin, X. A., Vázquez-Rodríguez, M., Rios, A. F., and Pérez, F. F.: Atmospheric CO_2 measurements and error analysis on seasonal air–sea CO_2 fluxes in the Bay of Biscay, J. Marine Syst., 66, 285–296, doi:10.1016/j.jmarsys.2006.05.010, 2007.

Padin, X. A., Castro, C. G., Ríos, A. F., and Pérez, F. F.: fCO_2^{sw} variability in the Bay of Biscay during ECO cruises, Cont. Shelf Res., 28, 904–914, 2008.

Padin, X. A., Navarro, G., Gilcoto, M., Rios, A. F., and Pérez, F. F.: Estimation of air–sea CO_2 fluxes in the Bay of Biscay based on empirical relationships and remotely sensed observations, J. Marine Syst. 75, 280–289, 2009.

Patra, P. K., Maksyutov, S., Ishizawa, M., Nakazawa, T., Takahashi, T., and Ukita, J.: Interannual and decadal changes in the sea-air CO_2 flux from atmospheric CO_2 inverse modeling, Global Biogeochem. Cy., 19, GB4013, doi:10.1029/2004GB002257, 2005.

Pérez, F., Padin, X. A., Pazos, Y., Gilcoto, M., Cabanas, M., Conde, P., Doval, M. D., and Farina-Busto, L.: Plankton response to weakening of the Iberian coastal upwelling, Glob. Change Biol., 16, 1258–1267, doi:10.1111/j.1365-2486.2009.02125.x, 2010.

Perissinotto, R., Laubscher, R. K., and McQuaid, C. D.: Marine productivity enhancement around Bouvet and the South Sandwich Islands (Southern Ocean), Mar. Ecol. Prog.-Ser., 88, 41–53, 1992.

Perissinotto, R., Lutjeharms, J. R. E., and van Ballegooyen, R. C.: Biological-physical interactions and pelagic productivity at the Prince Edward Island, Southern Ocean, J. Marine Syst., 24, 327–341, 2000.

Piola, A. R. and Rivas, A. L.: Corrientes en la Plataforma Continental en Boschi, EE (ed), El Mar Argentino y sus Recursos Pesqueros, Vol. 1: Antecedentes históricos de las exploraciones en el mar y las características ambientales, Instituto Nacional de Investigación y Desarrollo Pesquero, Mar del Plata, 119–132, 1997.

Poisson, A., Metzl, N., Brunet, C., Schauer, B., Bres, B., Ruíz-Pino, D., and Louanchi, F.: Variability of sources and sinks of CO_2 in the Western Indian and Southern Oceans during the year 1991, J. Geophys. Res., 98, 22759–22778, 1993.

Richardson, P. L. and McKee, T. K.: Average seasonal variation of the Atlantic Equatorial Currents from historical ship drifts, J. Phys. Oceanogr., 14, 1226–1238, 1984.

Richardson, P. and Reverdin, G.: Seasonal Cycle of Velocity in the Atlantic North Equatorial Countercurrent as Measured by Surface Drifters, Current Meters, and Ship Drifts, J. Geophys. Res., 92(C4), 3691–3708, 1987.

Romero, S. L., Piola, A. R. Charo, M., and García, C. E.: Chlorophylla variability off Patagonia based on SeaWiFS data, J. Geophys. Res., 111, C05021, doi:10.1029/2005JC003244, 2006.

Ríos, A. F., Pérez, F. F., and Fraga, F.: Water masses in the upper and middle North Atlantic Ocean east of the Azores, Deep-Sea Res. Pt. II, 39, 645–658, 1992.

Roy, C. and Reason, C.: ENSO related modulation of coastal upwelling in the eastern Atlantic, Prog. Oceanogr., 49, 245–255, 2001.

Roy, R., Rayner, P., Matear, R., and Francey, R.: Southern hemisphere ocean CO_2 uptake: reconciling atmospheric and oceanic estimates, Tellus B., 55(2), 701–710, 2003.

Sabine, C. L., Feely, R. A., Gruber, N., Key, R. M., Lee, K., Bullister, J. L., Wanninkhof, R., Wong, C. S., Wallace, D. W. R., Tilbrook, B., Millero, F. J., Peng, T. H., Kozyr, A., Ono, T., and Ríos, A. F.: The oceanic sink for anthropogenic CO_2, Science, 305, 5682, 367–371, 2004.

Santana-Casiano, J. M., González-Dávila, M., Rueda, M. J., Llinás, O., and González-Dávila, E. F.: The interannual variability of oceanic CO_2 parameters in the northeast Atlantic subtropical gyre at the ESTOC site, Global Biogeochem. Cy., 21, GB1015, doi:10.1029/2006GB002788, 2007.

Santos, A., Kazmin, A., and Peliz, A.: Decadal changes in the Canary upwelling system as revealed by satellite observations: Their impact on productivity, J. Marine Res., 63, 359–379, 2005.

Sarmiento, J. L. and Gruber, N.: Sinks for anthropogenic carbon, Physics Today, 55, 30–36, 2002.

Schuster, U. and Watson, A. J.: A variable and decreasing sink for atmospheric CO_2 in the North Atlantic, J. Geophys. Res., 112, C11006, doi:10.1029/2006JC003941, 2007.

Schuster, U., Watson, A. J., Bates, N., Corbière, A., Gonzalez-Davila, M., Metzl, N., Pierrot, D., and Santana-Casiano, M.: Trends in North Atlantic sea surface fCO_2 from 1990 to 2006, Deep-Sea Res. Pt. II, 56, 620–629, 2009.

Siedler, G., Laurence, A., and Müller, T. J.: Meddies and decadal changes at the Azores Front from 1980 to 2000, Deep Sea Res. Pt. II, 52, 583–604, 2005.

Siegenthaler, U. and Sarmiento, J. L.: Atmospheric carbon dioxide and the ocean, Nature, 365, 119–125, 1993.

Solomon, S., Qin, D., and Manning, M.: Climate Change 2007: The Physical Science Basis, Fourth IPCC Report, Cambridge Univ. Press, Cambridge, U. K., 2007.

Subramaniam, A., Yager, P. L., Carpenter, E. J., Mahaffey, C., Björkman, K., Cooley, S., Kustka, A. B., Montoya, J. P., Sañudo-Wilhelmy, S. A., and Shipe, R.: From the Cover: Amazon River enhances diazotrophy and carbon sequestration in the tropical North Atlantic Ocean, P. Natl. Acad. Sci. USA, 105, 10460–10465, 2008.

Takahashi, T.: Carbon dioxide in the atmosphere and in Atlantic ocean water, J. Geophys. Res., 66, 477–494, 1961.

Takahashi, T., Olafsson, J., Goddard, J. G., Chipman, D. W., and Sutherland, S. C.: Seasonal variation of CO_2 and nutrients in the high-latitude surface oceans: a comparative study, Global Biogeochem. Cy., 7, 843–878, 1993.

Takahashi, T., Sutherland, S. C., Wanninkhof, R., Sweeney, C., Feely, R. A., Chipman, D. W., Hales, B., Friederich, G., Chavez, F., Sabine, C., Watson, A. J., Bakker, D. C., Schuster, U., Metzl, N., Yoshikawa-Inoue,H., Ishii, M., Midorikawa, T., Nojiri, Y., K¨ ortzinger, A., Steinhoff, T., Hoppema, M., Olafsson, J., Arnarson, T. S., Tilbrook, B., Johannessen, T., Olsen, A.,, and Bellerby, R., Wong, C. S., Delille, B., Bates, N. R., and de Baar, H. J. W.: Climatological mean and decadal change in surface ocean pCO_2, and net sea-air CO_2 flux over the global oceans, Deep-Sea Res. Pt. II, 56, doi:10.1016/j.dsr2.2008.12.009, 2009.

Ternon, J. F., Oudot, C., Dessier, A., and Diverres, D.: A seasonal tropical sink for atmospheric CO_2 in the Atlantic ocean: the role of the Amazon River discharge, Mar. Chem. 68(3), 183–201, 2000.

Thomas, H., Bozec, Y., Elkalay, K., and De Baar, H. J. W.: Enhanced open ocean storage of CO_2 from shelf sea pumping, American Association for the Advancement of Science, 1005–1008, 2004.

Thomas, H., Prowe, A. E., Lima, I. D., Doney, S. C., Wanninkhof, R., Greatbatch, R. J., Schuster, U., and Corbière, A.: Changes in the North Atlantic Oscillation influence CO_2 uptake in the North Atlantic over the past two decades, Global Biogeochem. Cy., 22, GB4027, doi:10.1029/2007GB003167, 2008.

Ullman, D. J., McKinley, G. A., Bennington, V., and Dutkiewicz, S.: Trends in the North Atlantic carbon sink: 1992–2006, Global Biogeochem. Cy., 23, GB4011, doi:10.1029/2008GB003383, 2009.

Wanninkhof, R.: Relationship between wind speed and gas exchange over the ocean, J. Geophys. Res., 97, 7373–7382, 1992.

Wanninkhof, R., Olsen, A., and Trinanes, J.: Air–sea CO_2 fluxes in the Caribbean Sea from 2002–2004. J. Marine Syst. 66(1), 272–284, 2007.

Weiss, R. F.: Carbon dioxide in water and seawater: the solubility of non-ideal gas, Mar. Chem., 2, 203–215, 1974.

Wolf-Gladrow, D. A., Riebesell, U., Burkhardt, S., and Bijma, J.: Direct effects of CO_2 concentration on growth and isotopic composition of marine plankton, Tellus B, 51, 461–476, 1999.

Zeng, N.: Seasonal cycle and interannual variability in the Amazon hydrologic cycle, J. Geophys. Res., 104(D8), 9097–9106, 1999.